Sedimentology (2008) **55,** 499–530 doi: 10.1111/j.1365-3091.2007.00907.x

Tidal and seasonal controls in the formation of Late Miocene inclined heterolithic stratification deposits, western Amazonian foreland basin

JUSSI HOVIKOSKI*, MATTI RÄSÄNEN*, MURRAY GINGRAS†, ALCEU RANZI‡ and JANIRA MELO‡

**Department of Geology, University of Turku, 20014 Turku, Finland (E-mail: juanho@utu.fi)*

†Department of Earth & Atmospheric Sciences, 1-26 Earth Science Building, University of Alberta, Canada T6G 2E3

‡Laboratorio de Pesquisas Palaeontologicas, Departamento de Ciencias de Natureza, Universidade Federal do Acre (UFAC), 69.915-900 Rio Branco, Acre, Brazil

ABSTRACT

Upper Miocene strata in the Acre sub-basin, Brazil, consist dominantly of various types of inclined heterolithic stratification and pedogenic horizons. These strata were sedimentologically and ichnologically described to: (i) study different temporal controls responsible for inclined heterolithic stratification generation and their variation in a distal–proximal trend; and (ii) delineate the depositional setting. For this purpose, nine representative outcrops were sedimentologically and ichnologically studied, and their facies associations described. Thickness variations of the heterolithic strata of various orders (lamina, lamina bundles and beds) were analysed by statistical methods (Fourier transform). The deposits were interpreted as tidally and seasonally influenced estuarine or delta-related and continental strata. The inclined heterolithic stratification deposits represented vastly different settings ranging from tidally dominated, brackish-water ichnofossils-bearing channels to seasonally controlled, articulated *Purussaurus* (a freshwater alligator) fossil-bearing channels. Several time cycles were distinguished in the strata, including semi-diurnal, fortnightly and seasonal. Tidal imprint was best observed in low-energy brackish-water settings, whereas seasonal rhythmicity was distinguishable throughout the depositional system. However, the latter was most apparent in riverine channels proximal to the inferred fluvio-tidal transition. The different temporal controls commonly had distinguishable impact on sedimentological and ichnological properties in the studied sediments. The differing properties included: (i) the degree and nature of lateral variability with respect to lithology and bedforms in inclined heterolithic stratification; (ii) the lateral continuity of inclined heterolithic stratification; (iii) the nature of sedimentary contacts between the inclined heterolithic stratification members; (iv) thickness variation of inclined heterolithic stratification members within a set; (v) the cyclicities observed in inclined heterolithic stratification series; (vi) the degree of bioturbation; (vii) the types of trace fossils observed; and (viii) the distribution of bioturbation in adjacent inclined heterolithic stratification members.

Keywords Ichnology, inclined heterolithic stratification, Miocene, sedimentology, tidal deposits, tidal rhythmites, western Amazonia.

INTRODUCTION

This paper describes facies associations of upper Miocene strata in the Acre sub-basin, western Amazonian foreland basin, Brazil (Fig. 1). The facies associations mainly consist of various types of inclined heterolithic stratification (IHS of Thomas *et al.*, 1987) and pedogenic horizons that locally dominate the sedimentary record. IHS successions have received increasing attention recently because of their value as hydrocarbon source rocks (e.g. Athabasca Oil Sands, Canada). Most commonly, these successions have not only been interpreted as lateral accretion deposits of meandering fluvial or tidal channels and creeks (e.g. Thomas *et al.*, 1987; Page et al., 2003), but also as braided rivers, Gilbert-type deltas and elongate bars (Dalrymple *et al.*, 2003). Although no detailed comparisons between different IHS types have been made, it has been tentatively proposed that purely fluvial IHS may differ from their tidally influenced counterparts in that they possess more irregular bedding and dip angles (Thomas *et al.*, 1987). Moreover, IHS in Gilbert-type deltas differs from other IHS types by showing an upward-coarsening pattern.

The role of different temporal controls in IHS formation is also relatively poorly understood, and only few detailed studies on the subject exist. Notable exceptions include Gingras *et al.* (2002) and Lettley (2004). IHS formation is generally attributed to seasonal or random changes in the fluvial flow power in the continental settings, and seasonal and fortnightly migration of turbidity maxima in tidally influenced environments (e.g. Smith, 1988; Ainsworth & Walker, 1994; Bechtel *et al.*, 1994; Choi *et al.*, 2004).

This paper has two objectives. The first was to provide new knowledge of IHS development, particularly with regard to temporal controls and their variation in a distal (seaward) to proximal (continental) gradient. For this purpose, nine representative outcrops were sedimentologically and ichnologically studied, and their facies associations described (Fig. 1). The studied deposits provide exceptional insight into this issue because: (i) IHS deposits are diverse, reflecting both freshwater and brackish-water settings in the area; and (ii) typically, the deposits have good temporal resolution, allowing distinction of annual and tidal cycles. Sedimentological and ichnological responses to different temporal controls are compared, and some criteria are set out to distinguish them. This information is potentially useful in interpreting related deposits elsewhere.

The second purpose of the paper was to provide new palaeoenvironmental data for the Acre sub-basin Late Miocene, the depositional history of which is currently under debate. This paper is the first regional study based on these methods in the

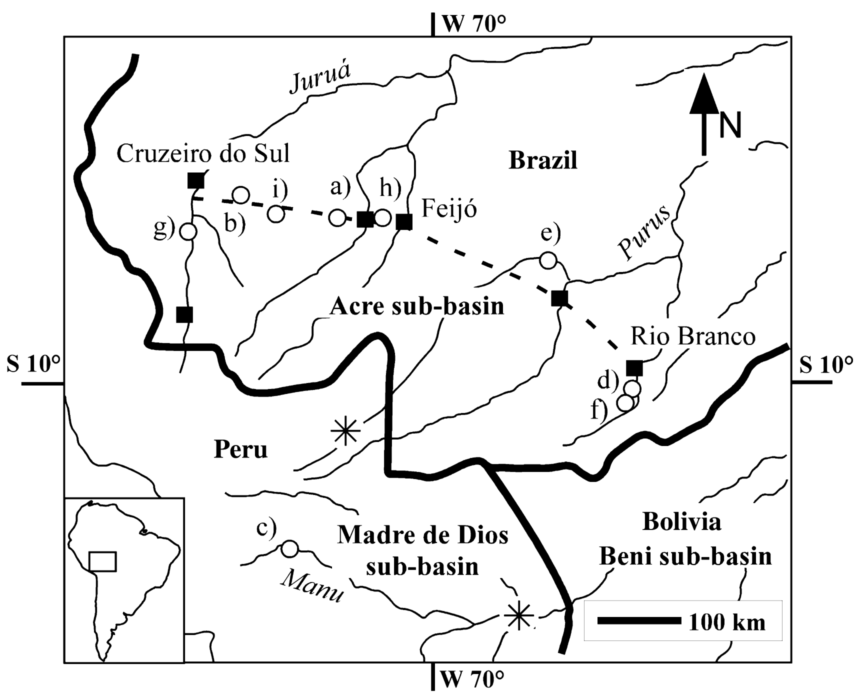

Fig. 1. Study locations: (a) Tarauacá, 16·5 km west of Tarauacá along BR 364; (b) Community Katukina (7°46′17″ S, 72°13′14″ W); (c) Cocha Cashu (11°54′11″ S, 71°23′39″ W); (d) Seringal Amapa (10°00′45″ S, 67°50′23″ W); (e) Talisma (approximately 8°47′27″ S, 68°49′43″ W); (f) Pavuna (approximately 9°55′40″ S, 67°52′55″ W); (g) Seringal Triunfo (8°47′1″ S, 72°49′59″ W); (h) Feijó; (i) Rio Liberdade (7°47′33″ S, 72°2′17″ W); Star, tuff implying Late Miocene age (Campbell *et al.*, 2001; Hermoza, 2004); dashed line, road BR 364; thick solid line, country border.

area, which was previously studied by various palaeontological field parties (see below). Some previous local case studies proposed tidal influence in these strata (Acre sub-basin: Räsänen *et al.*, 1995; Gingras *et al.*, 2002; Madre de Dios sub-basin: Hovikoski *et al.*, 2005). However, the idea of marginal marine influence has not generally been accepted for the Acre sub-basin. The arguments used against tidal affinity involve fossil data rich in terrestrial vertebrates, including ancient freshwater turtles, and fish that are typical of modern Amazonian flood plains (Frailey, 1986; Paxton & Crampton, 1996; Latrubesse *et al.*, 1997; Carvalho *et al.*, 2002; Brito & Deynat, 2004). Less typical finds for Amazonian taxa include euryhaline fossils such as bullshark teeth (e.g. Räsänen *et al.*, 1995). The area had also developed a seasonal climate by the Miocene (Kaandorp *et al.*, 2005). It was hypothesized that seasonally induced variations in fluvial flow power could have produced the observable heterolithic patterns (Hoorn, 1996; Paxton & Crampton, 1996; Westaway, 2006). Recently, Gingras *et al.* (2002) reported annual cyclicity in brackish-water ichnofossils bearing an IHS channel from the southern part of the Acre sub-basin. Finally, no diagnostic properties for tidal deposits, such as high certainty cyclic rhythmites clearly attributable to neap–spring cycles, were previously reported for Acre. Distinguishing between tidal and seasonal rhythms would contribute to the understanding of Amazonian palaeogeographical development and consequently provide information, for example, for phylogenetical studies of Amazonian aquatic taxa.

STUDY AREA

The Acre sub-basin is located in western Brazil, in the Acre state (Fig. 1). Together with the Madre de Dios-Beni sub-basin, it forms the southern end of the western Amazonian foreland basin covering roughly 5×10^5 km^2. This paper reports on eight river and road outcrops within the Acre sub-basin (Fig. 1). The data are complemented by observations from an outcrop of the adjacent Madre de Dios (Peru) sub-basin. The deposits belong to the upper part of the Solimões Formation in Brazil (e.g. Schobbenhaus *et al.*, 1984), whereas the Peruvian deposits are informally known as the Ipururo Formation and the Madre de Dios Formation (Kummel, 1948 and Oppenheim, 1946, respectively). In this study, all the reported sediments are included into the Solimões Formation because they are lithologically similar, part of the same depositional system, and represent roughly the same stratigraphic level (see below). The thickness of the Miocene sedimentary succession is about 350 m near Acre (Hoorn, 1994).

No exact correlation is possible between the outcrops. However, all the sediments studied are estimated to be Late Miocene in age based on their: (i) stratigraphic position; (ii) fossil content; and (iii) isotope ages. These strata overlie the Pebas Formation, which is estimated to be late Early to early Late Miocene in age based on the pollen zonation of Hoorn (1994). So far, no published pollen results are available from the Acre or Madre de Dios deposits. The occasionally discovered mollusc fossils represent a post-Pebas fauna in both basins and thus confirm the stratigraphic location of the deposits (Wesselingh, 2003). Moreover, the rich vertebrate fossils point generally to the Late Miocene (Huayaquerian land mammal age) (e.g. Frailey, 1986). Finally, ^{40}Ar/^{39}Ar dates from several tuff layers in Madre de Dios imply an age of 9 to 3 Myr for the time of deposition (Campbell *et al.*, 2001; Hermoza, 2004; Fig. 1).

METHODS

The basic data set consists of sedimentological and ichnological field descriptions. Grain-size, sedimentary structures, palaeocurrent directions (measured from ripple and dune foresets), nature of bedding, bedding contacts and lateral variability were described. The sedimentological approach also includes an analysis of thickness data for heterolithic deposits of various orders. Thickness variations of sand-clay or silt-clay couplets were calculated from lamina rhythmites, lamina bundles and bed successions; these were interpreted as semi-daily/daily, neap–spring and seasonal deposits respectively. Figures 10C and 13D illustrate how the lower frequency couplets are constructed. These data were analysed with the spectral procedure of SAS 8.2 (finite Fourier transform) to identify possible cyclicities. The possible sources of error are: (i) in places there are signs of erosion in some mud drapes; (ii) the mud drapes are not well-developed everywhere (thin, discontinuous); and (iii) sand laminae are locally absent in the low-energy phases. Locally, poor preservation and imperfect lamina development may hinder recognition of individual sand-clay lamina couplets. Finally, delineation of a couplet in the lower frequency examples was subjective where the IHS members were truncated. The number of couplets in Fig. 10F may be slightly higher or lower in reality.

The ichnological approach included documentation of the recognized ichnogenera, interpretation of their ethology, dimensions of the traces and estimation of bioturbation intensity.

INCLINED HETEROLITHIC STRATIFICATION FACIES

Below is a brief synthesis of common facies types of the Upper Miocene strata in the Acre sub-basin. This discussion is followed by a more detailed account of sedimentological and ichnological characteristics of IHS deposits.

Overview of facies

The described deposits formed sharp-based, upward-fining IHS successions. These strata were typically interbedded with root-bearing mud or pedogenically altered mud. In places, unionid bivalves were present in the root-bearing mud (cf. Wesselingh, 2003). In some outcrops, this facies formed much of the stratigraphic record. Other observed facies that occurred adjacent to the IHS strata included horizontally bedded, current ripple-bearing sand and laminated mud. These strata were continuous laterally, formed some tens of centimetres thick couplets, and contained local occurrences of *Planolites* and synaeresis cracks. Also present are *Thalassinoides*-bearing well-sorted, sand facies. Finally, sharp-based, homolithic, upward-fining successions are present locally.

The studied IHS successions were sedimentologically and ichnologically diverse. The differences included lateral continuity of IHS, couplet thickness, frequency of lithological heterogeneities, type of bioturbation and its distribution and fossil content. Particularly based on the above-mentioned sedimentological criteria, the studied IHS successions can be divided into four broad IHS facies associations (FA1 to FA4). Each facies association type bears ichnological, sedimentological and palaeontological variability and, therefore, the facies associations are further divided into sub-facies associations. These sub-facies associations are described in Tables 1 to 4. In the text below, the generalized, four facies associations are described and interpreted.

Facies Association 1 (localities A and B-Fig. 1)

Facies Association 1 forms sharp-based, 8 to 12 m high, generally upward-fining successions. It is gradationally capped by a pedogenic horizon or FA2, and sharply overlies FA4. The sharp lower contact of FA1 is gently inclined, irregular and bears mud-clasts. Characteristic features of FA1 are shown in Fig. 2 and include: (i) the deposits form composite sets (inclined stratification [IS]-IHS); (ii) relatively thick IHS successions and individual couplets; (iii) low number (approximately five) of couplets in a set; (iv) laterally extensive IHS members; (v) presence of higher frequency lithological heterogeneities that display poorly cyclic rhythmites; and (vi) *Skolithos*-bearing mud drapes. FA1 was divided into two sub-facies associations, FA1a (Figs 3 to 5) and FA1b (Figs 6 to 8), mainly based on ichnological criteria (Table 1).

FA1: Cross-stratified silty sand, inclined stratified mud and sand

Sedimentological characteristics. The IS-set consists of trough-cross-stratified or low-angle, planar-stratified silty sand. The dunes are most commonly 10 to 30 cm high (highest 70 cm), and as cosets they form 1 to 3·5 m high compound units. The dune bottomsets form massive mud beds a few centimetres thick at various inclinations, which can be followed laterally up to several metres (Fig. 5A and B). Where observed, the width of the larger troughs was typically more than 5 m (FA1b). The cross-strata are commonly mud draped, or bear minute, mud-draped ripples (Figs 5C and 8A). Double mud drapes are present regularly in FA1b (Fig. 8F). Laterally, the IS-set is continuous and can be followed for over 50 m. Upward, the deposits grade into ripple-cross-stratified or massive, very fine-grained sand which comprises coarse members in IHS.

The IHS set consists of coarse-to-fine couplets. The members are cross-stratified or massive silty sand (Figs 5E and 8E), and inclined, laminated or bioturbated mud (Fig. 8B and E). The thickness of the members varies between the sub-facies associations: in FA1a, the thickness of the coarse member is 10 to 30 cm, whereas the fine member is 2 to 30 cm thick. In FA1b, the coarse member can be 0·5 to 2 m thick and the fine member 20 to 60 cm thick. In both cases, the contact from coarse to fine is sharp, although the grain-size change is slightly gradational

Table 1. Summary of FA1a and FA1b.

Facies Association FA1	Occurrence	Sedimentology of IS	Sedimentology of IHS	Ichnology of IS	Ichnology of IHS	Interpretation
FA1a (Fig. 5A–G) Trough-cross-stratified bioturbated silty sand (IS), and inclined, massive sand and bioturbated mud (IHS)	Stratigraphically above FA4 in erosion, gradationally below a pedogenic horizon. Forms upward-fining successions 8 m thick. Lower contact: sharp, gently inclined mud-clast-bearing surface	Trough cross-stratified silty sand 3·5 m thick. Superimposed current ripples and mud drapes on strata. Well-developed muddy bottomset in 3D dunes. Mud-pebble beds occur at the bottom of the facies. Lateral continuity: at least 50 m	Coarse member: massive muddy sand 10 to 30 cm thick. Fine member: laminated or massive mud 2 to 30 cm thick. Both contacts between members sharp. Apparent dip 10° to 20°. Lateral continuity: at least some tens of metres	Low bioturbation intensity. Simple tier suites of morphologically simple, shallow tier traces descending from mud drapes (lined Sk, Pl). Dune bottomset intensively reworked by La, Pl, lined Sk, lined Ps	Fine member: reworked by La, Pl and Sk. Variable bioturbation intensity (10% to 100%). Coarse member: low bioturbation intensity. Eq/fu in places	Upper LFR current velocity with regularly occurring stillstands. Rapid changes from traction to suspension. Brief time cycle (hour scale) associated with the mud drapes. Tidally influenced, seasonally dominated. ?Mesohaline. Estuarine point bar
FA1b (Fig. 8A–E) Cross-stratified silty sand (IS), and inclined sand and laminated mud (IHS)	Stratigraphically above FA4 in erosion, below FA2a in gradation. Total thickness: 12 m. Form upward-fining successions 5 m thick. Lower contact: irregular, nearly horizontal mud-clast-bearing surface	Trough-cross-stratified or plane-parallel-stratified silty sand 1 to 2 m thick. Superimposed current ripples and double mud drapes on strata. Bear poorly cyclic rhythmites (a cycle comprises of 15 to 21 couplets, $n = 3$). Lateral continuity: at least 70 m	Coarse member: ripple-cross-stratified silty sand 1 to 2 m thick. Mud-draped climbing ripples common. Fine member: interlaminated mud bed 20 to 60 cm thick. Form intraformational breccia in a down-dip direction. Double-mud drapes. Poorly cyclic rhythmites. Apparent dip 5° to 20°. Contacts: gradational from coarse-to-fine, sharp from fine to coarse. Lateral continuity: at least 70 m	Low bioturbation intensity. Simple tier suites of morphologically simple, shallow tier traces descending from mud drapes (Sk, Pl)	Fine member: small-scale burrow mottling in clay lamina. Coarse member: low intensity suites consisting of Pl, Sk and Ta	Upper LFR to UFR current velocity with regularly occurring stillstands. Rapid changes from traction to suspension. Brief time cycle (hour-scale) associated with the mud drapes. Tidally influenced, seasonally dominated. Low-salinity to freshwater deposits. Deltaic channel

[LFR = lower flow regime; UFR = upper flow regime].

Table 2. Summary of FA2a and FA2b.

Facies Association FA2	Occurrence	Sedimentology	Ichnology	Interpretation
FA2a (Fig. 10A–H) Inclined, bioturbated ripple-cross-stratified sandy silt, laminated mud and rooted mud (IHS)	Stratigraphically above FA1a in gradation, below a pedogenic horizon in gradation. An upward-fining succession 3 m thick. Part of a 12 m thick succession. Lateral continuity: limited, few tens of metres in maximum except for rooted mud which can be followed up to 70 m	Coarse member: mud-draped current ripples 0·5 to 5 cm thick. Fine member: interlaminated mud and silty sand 1 to 5 cm thick. Contacts between members bigradational. Rapid lateral changes in lithology and bedforms. True dip *ca* 10° to 15°. Cyclic rhythmites, asymmetric couplets. Bipolar palaeocurrent directions. Also, a lower frequency facies occurs: rooted, massive mud 5 to 25 cm thick. Vertical spacing 1 to 1·5 m. Lower contact gradational, upper sharp	Moderate-to-low bioturbation intensity. Low-diversity suites comprising La, Lo, Pa, Th/Pl, fu, eq, on the top Ta. Diminutive Pl in rooted mud	Regular changes in flow velocity. Rapid depositional rate. Combined traction and suspension. Tidally dominated. Brackish water. Abandoned deltaic channel infilled with lower energy estuarine deposits
FA2b (Fig. 11A–D) Inclined, climbing-ripple-bearing sand and interlaminated mud and sand (IHS)	Stratigraphically interbedded with the same FA (FA2b) or a pedogenic horizon. Lower contact sharp An upward-fining succession 3 m thick. Imbricate cosets. Lateral continuity: less than 10 m	Coarse member: mud-draped, climbing ripple-bearing sand 4 to 8 cm thick. Fine member: interlaminated mud and sand or massive mud 3 to 5 cm thick. Contacts between members bigradational. Rapid lateral changes in lithology and bedforms. Apparent dip 10° (constant). Bipolar palaeocurrent directions. Cyclic rhythmites. 'Synaeresis' cracks	Mainly unburrowed. Some bedding plane traces occur: Un in pinstripe mud. Also, Di and ?Ph are present in adjacent rhythmite facies	Regular changes in flow velocity. Rapid depositional rate. Combined traction and suspension. Tidally dominated. Fluctuating salinity-freshwater? Sub-tidal creek

Table 3. Summary of FA3a and FA3b.

Facies Association FA3	Occurrence	Sedimentology of IHS	Ichnology of IHS	Interpretation
FA3a (Fig. 13B) Inclined, mud-draped, ripple cross-stratified fine-grained sand and inclined, massive or laminated clayey mud	Stratigraphically below a pedogenically altered horizon in gradation, or a sharp-based, upward-fining succession. Lower contact: erosional and bears mud-clasts. Forms upward-fining successions 8 m thick. Imbricate cosets. Lateral continuity: at least 60 m	Coarse member: mud-draped current ripples. Coset thickness 2 cm to 2 m. Fine member: laminated or massive mud 2 to 30 cm thick. Great number of mud-lamina in one couplet. True dip: 15 to 20° (flattens out in up-dip direction). Contacts between members: gradational or sharp from coarse to fine, sharp from fine to coarse. Beds are fully contorted in a down-dip direction in places. Couplets can form non-random series	Low bioturbation intensity. Sporadic, monospecific Cy in coarse member. Rare assemblages of Pl, Sk or Ar	Lower LFR flow velocity. Regular, high-frequency pulses in hydrodynamic energy. Tidally influenced, seasonally dominated. Fluctuating, low salinity. Fluvio-tidal point bar
FA3b (Fig. 13C and D) Inclined, ripple cross-stratified fine-grained sand and inclined massive or laminated clayey mud	As above	As above, the differences are: Coarse member: current-rippled fine-grained sand. No higher frequency lithological heterogeneities present. Adjacent coarse-to-fine couplets are asymmetric repeatedly. Couplets may form random series. Gypsum crystals in places	From very low bioturbation intensity to unburrowed. Rare assemblages of Pl, Ta, unlined Sk or Ar. Side-necked turtle fossil discovered at locality D (Carvalho *et al.*, 2002)	Lower LFR flow velocity. Seasonally dominated. Freshwater. Fluvio-tidal point bar

Table 4. Summary of FA4a to d.

Facies Association FA4	Occurrence	Sedimentology	Ichnology/fossils	Interpretation
FA4a (Fig. 15A–C) Inclined, bioturbated sandy mud and root bearing mud (IHS)	Stratigraphically below FA1 in erosion. Lower contact: not visible. Upward fining succession 2 m thick. Lateral continuity: at least 10 m (limited by an erosional surface)	Coarse member: massive, greyish mud 20 to 40 cm thick. Fine member: massive, reddish, root-bearing mud up to 15 cm thick. Contacts between members: gradational (bioturbated) from fine to coarse, sharp from coarse to fine. Apparent dip 15° to 20° (flattens out in up-dip direction). Couplets show irregular thickness variation. The beds contain faults up to 20 cm deep	Coarse member: low-diversity suites of small Pa and Gy. Moderate or low bioturbation intensity (up to 50%). Fine member: monospecific suites of meniscus bearing burrows (various sizes) and roots. Very low bioturbation intensity (approximately 10%)	Alternation of sub-aerial and sub-aqueous conditions. Seasonal cyclicity. Very low energy Fluctuating, low salinity. Proximal intertidal creek
FA4b (Fig. 15D–F) Inclined, massive or stratified muddy sand and massive marly mud (IHS)	Stratigraphically below a pedogenic horizon in gradation. Lower contact: not visible. Upward-fining succession 2·5 m thick. Lateral continuity: at least 25 m (limited by the current erosional surface)	Coarse member: massive or trough-cross-stratified muddy sand 20 to 60 cm thick. Water escape structures in places. Fine member: apparently massive marly mud *ca* 5 cm thick. Contacts between members: interlayered from coarse-to-fine, sharp from fine to coarse. Apparent dip 10° to 20° (obscured by post-depositional deformation)	Low to high bioturbation intensity. Coarse member: meniscus bearing burrows of various sizes and diminutive Pl, Ps, ?Gy. Fine member: passively filled, deeply penetrating, unlined, burrow complexes and roots descend from the fine member. The burrow complexes are reburrowed by diminutive Pl in places	Alternation of sub-aerial and sub-aqueous conditions. Seasonal cyclicity. low-salinity?-freshwater Proximal, intertidal creek
FA4c Inclined massive mud and organic rich mud (IHS)	Stratigraphically in-between pedogenic horizons. Lower contact: laterally limited, inclined erosional surface. Upward-fining succession 4 m thick. Lateral continuity: *ca* 10 m (limited by an erosional surface)	Coarse member: apparently massive. Dark brown. Fine member: apparently massive. Contacts between both members sharp. IHS attached to the base of the succession. No higher frequency lithological heterogeneities observed. Apparent dip up to 30°	No trace fossils observed. Articulated Purussaurus fossil was discovered in FA4c near location H	Seasonal cyclicity. Very low energy. Freshwater. Riverine creek

Table 4. (*Continued*)

Facies Association FA4	Occurrence	Sedimentology	Ichnology/fossils	Interpretation
FA4d (Fig. 15G) Inclined, stratified sandy silt and desiccation crack bearing mud (IHS)	Stratigraphically interbedded with the same FA (FA4d) or grades into a pedogenic horizon Lower contact: erosional. Forms upward-fining successions 3 m thick. Lateral continuity: several tens of metres	Coarse member: massive or laminated, sandy mud. Fine member: massive or laminated, root and desiccation crack bearing mud. Contacts between members: gradational from coarse-to-fine, sharp from fine-to-coarse. Couplets normally graded 30 to 80 cm thick: no distinct members in places. Occasional load casts and water escape structures. Up to 80 cm deep desiccation cracks from fine member. True dip: 5° to 10°, occasionally more	Rare meniscus-bearing burrows and root bioturbation especially near the top of the succession. Burrow mottling in places	Alternation of sub-aerial and sub-aqueous conditions. Seasonal cyclicity. Very low energy. Freshwater. Ephemeral, riverine creek

(normally graded) (Fig. 8E). The contact from fine to coarse is sharp and commonly truncated. The fine members form intraformational breccia, and grade into IS in the down-dip direction. The lateral continuity of the IHS is uncertain due to post-depositional pedogenic overprints, but the discontinuous beds can be followed up to at least from a few tens of metres to 70 m. The apparent dip of the beds is 5° to 20°. Both the IS and IHS sets may bear poorly cyclic rhythmites (a cycle comprising 15 to 21 couplets, $n = 5$). Palaeocurrent measurements are illustrated by rose diagrams in Figs 3, 4 and 7.

Ichnological characteristics. The two sub-facies associations bear ichnological differences. In both cases, the degree of bioturbation and ichnogenera diversities are generally low in IS. Rare, vertically oriented, robust equilibrium structures occur in FA1a (Fig. 5B). However, the muddy dune bottomsets are, in places, moderately to fully reworked by horizontally oriented *Laminites* (Fig. 5C and D) and *Planolites*. *Planolites* cross-cut *Laminites*. Also locally present are mud-lined, I-shaped, 1 to 2 cm wide, vertical burrows (possibly *Psilonichnus*, Fig. 5C; cf. Nesbitt & Campbell, 2006) and actively mud-filled, vertical, unlined probing traces (1·5 cm in diameter) of unknown ichnotaxonomic affinity. In addition, low-density suites of *Skolithos* and *Planolites* dip down from the mud drapes or follow them infaunally in both the sub-facies associations (Figs 5C and 8C,D). Also present in FA1b are *Palaeophycus* and *Taenidium*. No cross-cutting of trace fossils was observed.

Bioturbation is concentrated in one of the members in IHS. In FA1a, bioturbation intensity varies from 10% to 80% in the fine member. The coarse member hosts a lower degree of bioturbation (<20%). As with the IS-set, the ichnofabric is *Laminites* dominated (Fig. 5E).

In FA1b, the fine member bears very low bioturbation intensity and diversity. Sporadic, small-scale burrow mottling is observed in clayey lamina (Fig. 8B and E). The coarse member is ichnologically similar to the IS-set. Finally, an assemblage of irregular burrows with thinner branches, thin vertical shafts with bulbous enlargements and meniscae-bearing traces burrow the rippled mud in the top of the FA in places (Fig. 5F and G). The infill of these burrows is derived from the overlying, pedogenically altered material.

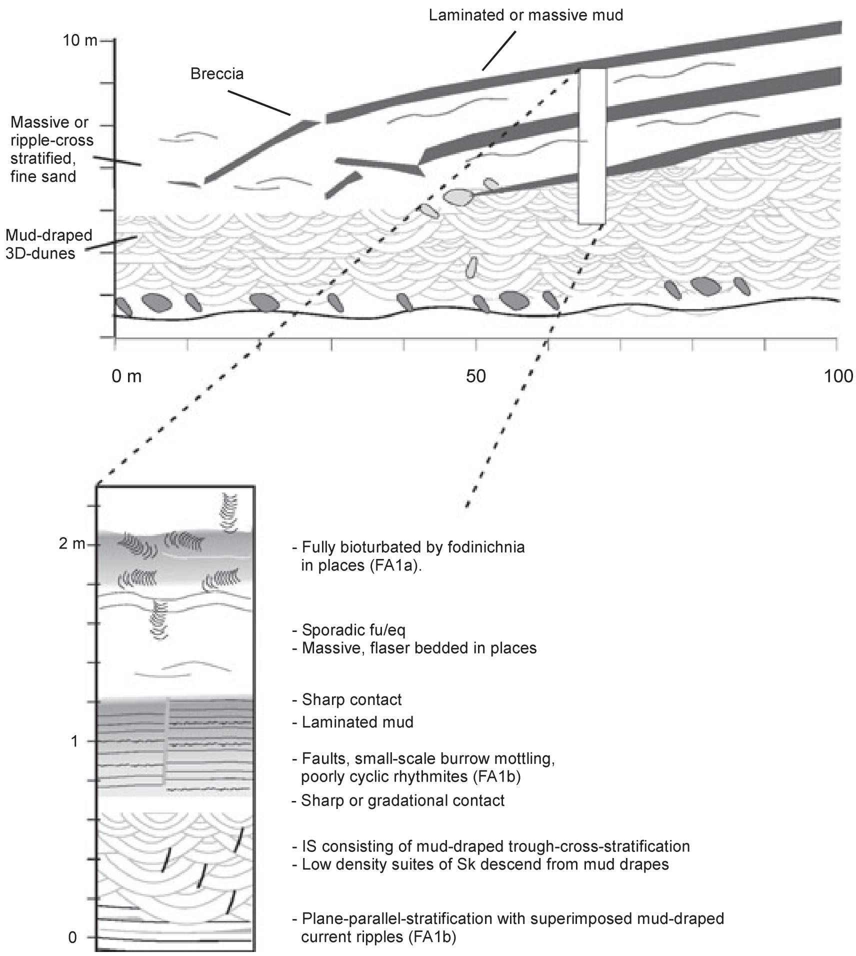

Fig. 2. Generalized schematic view of FA1. Main sedimentological and ichnological characteristics are shown [Fu = Fugichnia; eq = equilibrichnia; Sk = *Skolithos*].

Interpretation of FA1

The upward-fining succession with a truncated, sharp base is best explained by a channel environment. In addition to the general upward-fining character of the succession, the palaeocurrent directions change slightly upward within the set (Fig. 7), pointing to a meandering, low-sinuosity channel. The IS-set directly overlies the mud-clast-bearing lower contact and, therefore, is interpreted as a mid-channel, lower point bar deposit; the IHS set is most readily explained as channel-margin deposits.

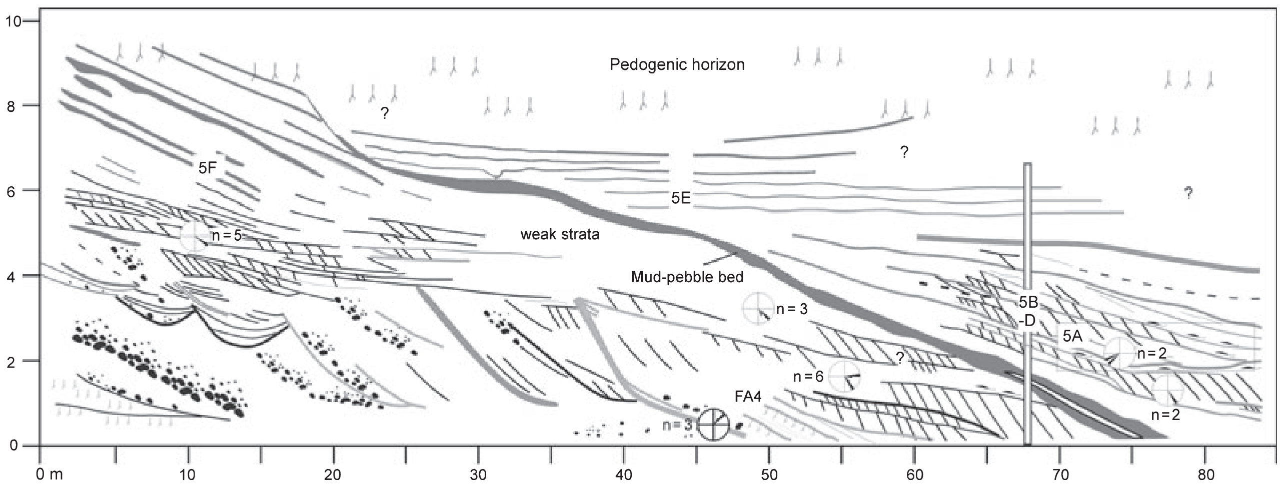

Fig. 3. Schematic view of FA1a. Numbers and letters indicate locations of respective figures. Black-lined white bar shows the locality of the log profile (Fig. 4).

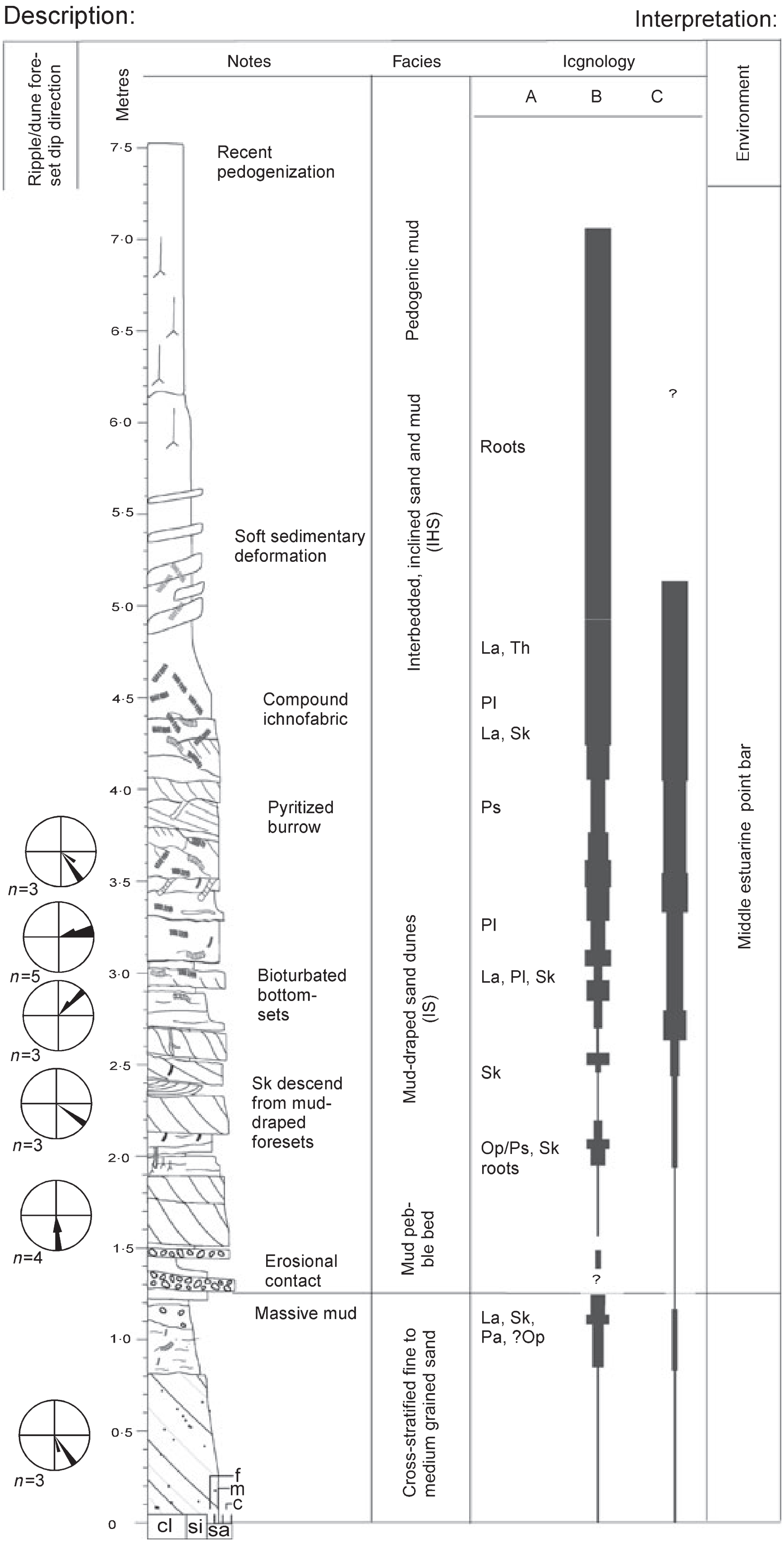

Fig. 4. Log profile of FA1a. Ichnological abbreviations are explained in Fig. 7.

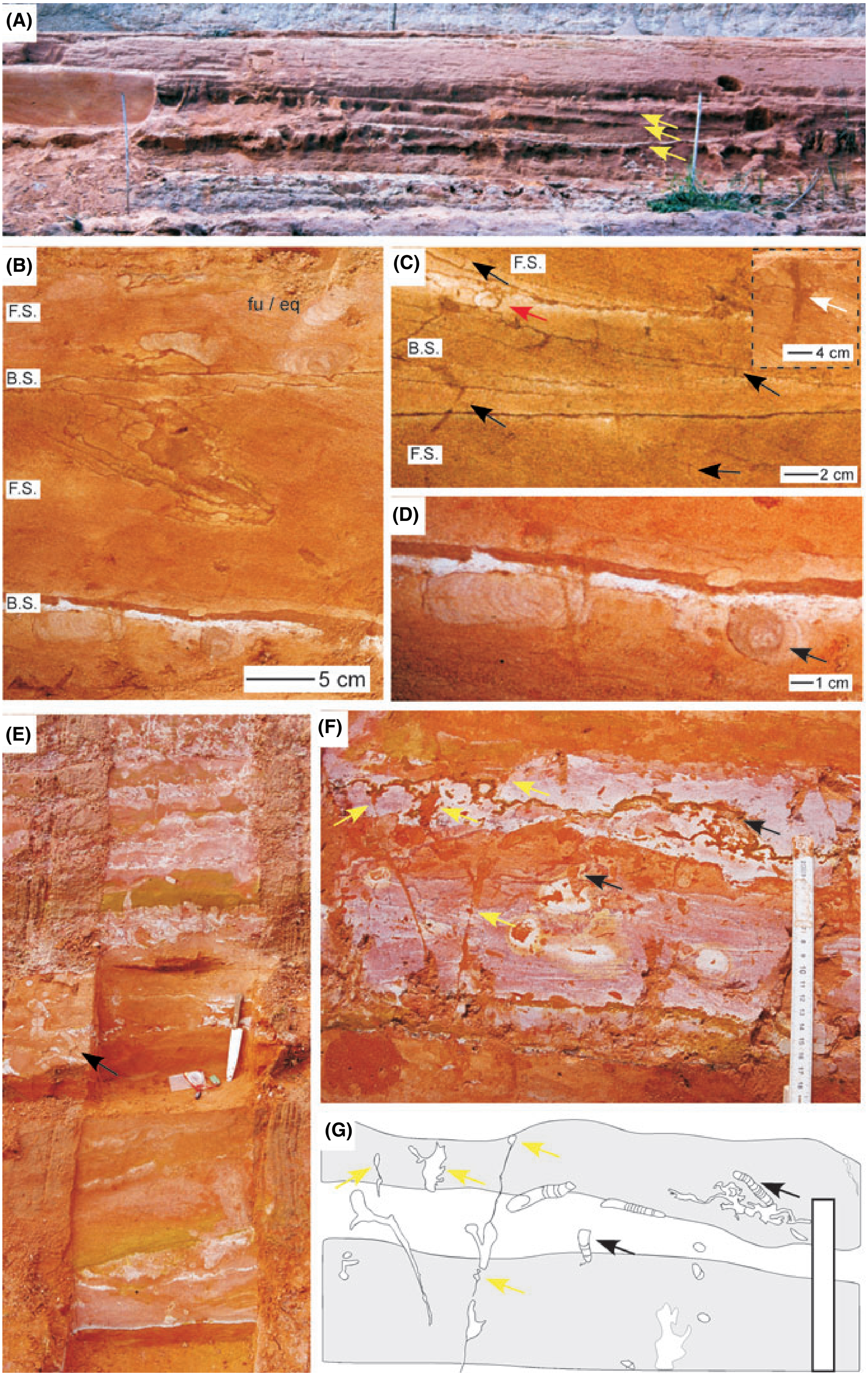
(A)
(B)
F.S.
fu / eq
B.S.
F.S.
B.S.
5 cm
(C)
F.S.
B.S.
4 cm
F.S.
2 cm
(D)
1 cm
(E)
(F)
(G)

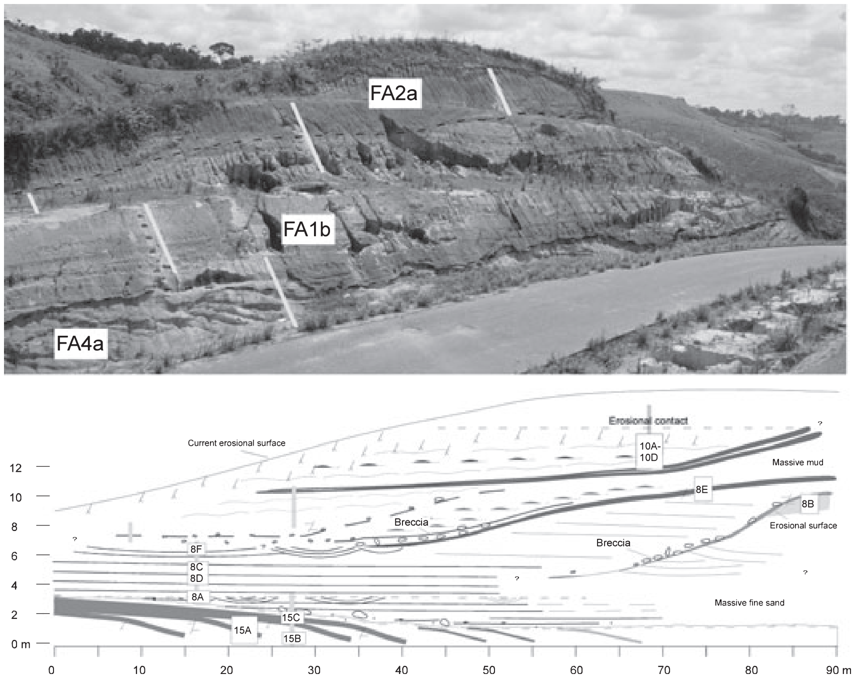

Fig. 6. A photograph and schematic view of locality A. Numbers and letters point to locations of respective figures. Grey bars indicate composite log locations.

FA1 is interpreted as being tidally influenced for several reasons. Initially, the bedforms reflect rapid changes in flow velocities. Undulating or rippled clay drapes are superimposed on Upper Flow Regime (UFR) plane-parallel lamination and upper Lower Flow Regime (LFR) trough cross-stratification (cf. Allen, 1968). Furthermore, the deposits generally lack bioturbation, but low-density suites of morphologically simple, shallow tier traces biogenically modify the mud drapes (Figs 5C and 8B to D). This concentration of deposit-feeding activities probably indicates nutrient concentration resulting from organic debris fallout during quiescent periods; it also implies a brief slack-water period for clay drape formation (colonization window of Pollard *et al.*, 1993). Finally, adjacent sand-clay couplets of FA1a show, in places, thick–thin alternations probably indicating the influence of semi-diurnal processes (Fig. 8F; de Boer *et al.*, 1989). In concert, the above-mentioned factors point to an environment that was subject to regular, high-frequency changes in hydrodynamic flow power.

The primary control in the IHS formation in FA1 is inferred to be annual. This interpretation is based on the great number of couplets in both members (FA1a); they probably consist of several, amalgamated neap–spring cycles (Fig. 8B). The annual inference is further supported by the thickness of the members. Couplet thickness reaches up to 60 cm in FA1a, and over 2 m in FA1b; that would be an anomalously high depositional rate for fortnightly deposits (up to 20 cm in a day) and almost certainly would hinder the existence of an endobenthic community. However, the depositional parameters allowed permanent colonization of a low-density and diversity, simple tier infaunal community in the channel. The fine member is interpreted as representing dry seasonal conditions, because its vertical equivalent in FA2a bears roots (see FA2 for discussion). The low bioturbation intensities in the FA1b fine member probably point to increased turbidity stress during the dry season. Fine-grained members correlate lithologically to the trough-cross-stratified part of the IS-set in

Fig. 5. FA1a. (A) Overview to IS-set. Yellow arrows, muddy dune bottomsets. (B) A close-up to IS. Note the change in orientation in trace fossils in transition from bottomset to foreset. [B.S. = bottomset; F.S. = foreset; La = *Laminites*; eq = equilibrichnia; fu = fugichnia.] (C) Close-up to mud-draped dune foresets–bottomsets and associated bioturbation. Black arrow, *Skolithos* descending from mud-draped strata; Red arrow, *Laminites*; white arrow in insert indicates mud-lined ?*Psilonichnus* descending from bottomset. (D) Close-up to *Laminites* at sand–mud interface. (E) Interbedded, inclined massive sand and mud (IHS). Fine member is fully bioturbated in places. Black arrow indicates dense *Laminites* fabric. Compass as a scale (12 cm long). (F) An assemblage of irregular burrows and meniscae-bearing trace fossils from the top of FA1a. Black arrows, Meniscae-bearing burrows; yellow arrows, chambers and galleries in vertical shafts. Ruler as a scale (15 mm wide). (G) Schematic interpretation of Fig. 5F.

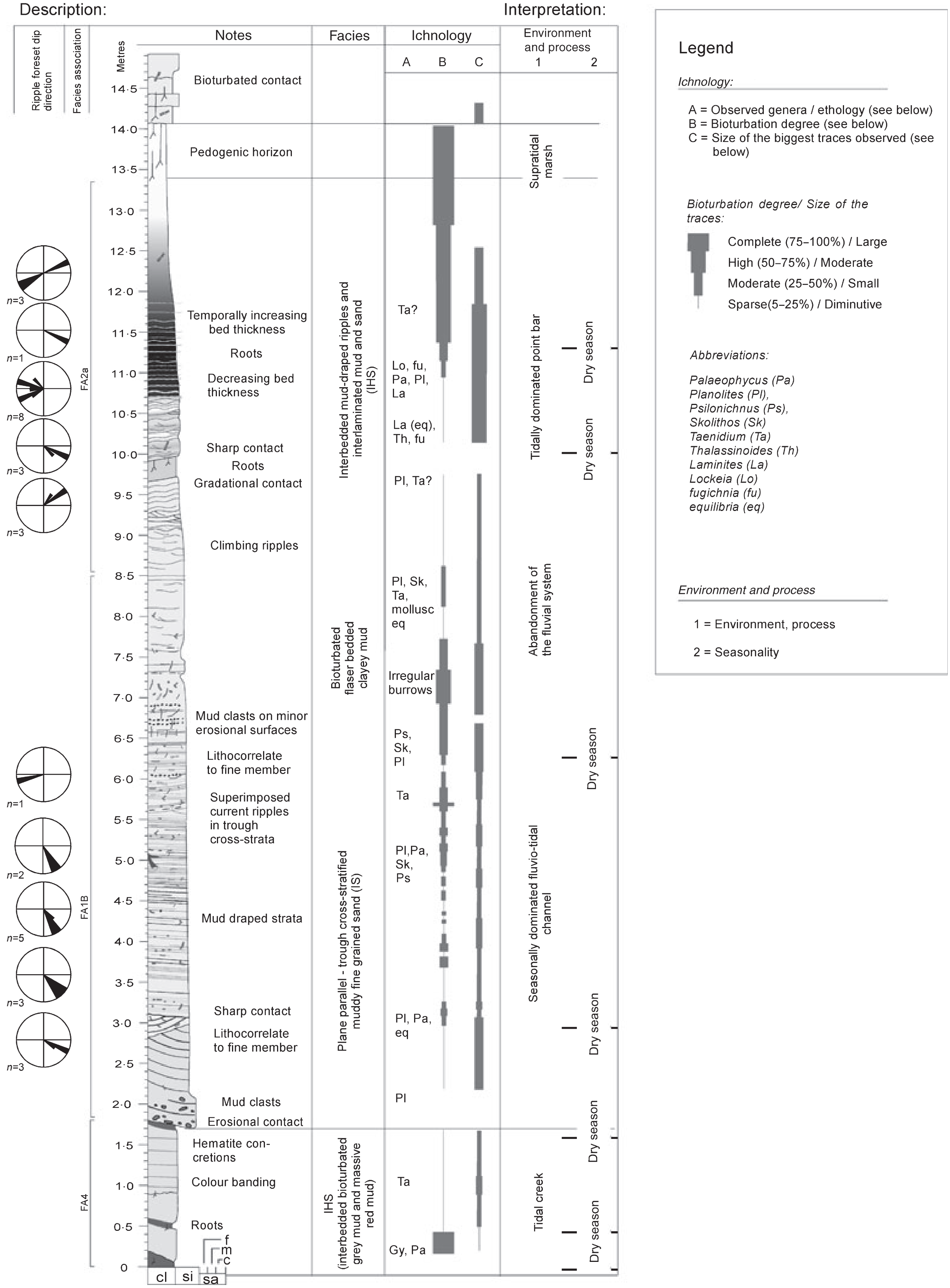

Fig. 7. Composite log profile from location A. Facies Associations 1b, 2a and 4a are shown.

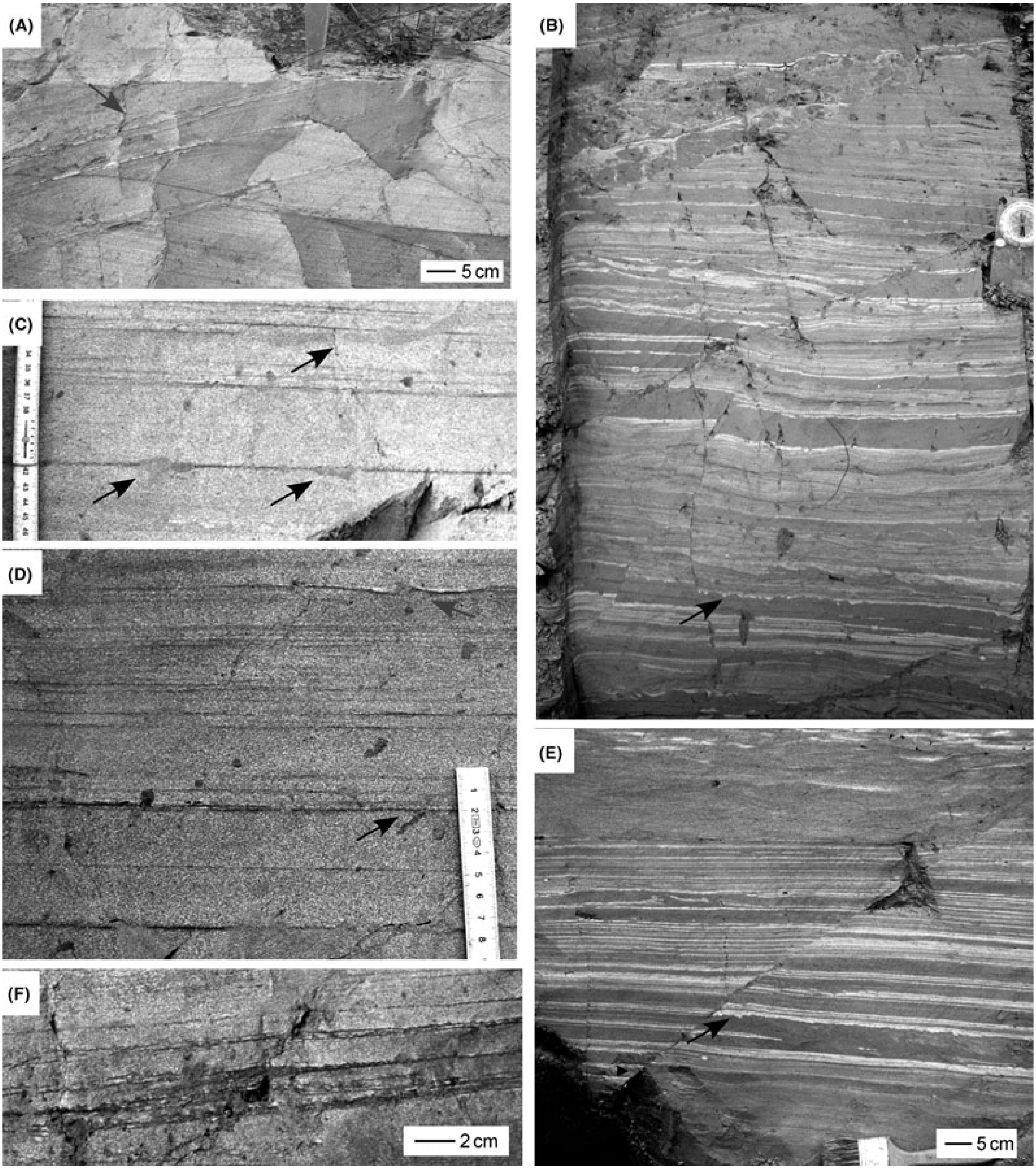

Fig. 8. FA1b. (A) Trough-cross-stratified sand-forming IS. Black arrow, superimposed, mud-draped current ripple. (B) Vertically stacked, non-cyclic silty rhythmites forming IHS fine member. Black arrow, small-scale burrow mottling. Compass as a scale (12 cm long). (C) Mud-draped strata. Black arrows, *Planolites* burrowing mud drapes. Ruler as a scale (15 mm wide). (D) Plane-parallel stratification. The strata are, in places, mud draped. Black arrow, *Skolithos* descending from a mud drape. Grey arrow, mud-draped current ripple. Ruler as a scale (15 mm wide). (E) Silty rhythmites (fine member). Note the gradational lower contact and sharp upper contact of the bed. (F) Close-up of large-scale trough-cross-stratification forming coarse member. The mud-draped strata form double mud drapes.

FA1b; this further suggests that, during the dry season, the flow velocities drop and consequently that the mid-channel was ebb dominated.

In FA1a, there is no conclusive evidence of a time cycle responsible for the generation of the prominent bottomset–foresets alternation in IS. The foresets are, in places, too faint to enable calculation of the exact number of events in each cycle. Patchy high bioturbation intensity and compound ichnofabrics in tens of centimetre-thick sets, and sporadic roots associated with the bottomsets, probably require more than seven days to develop.

FA1a is interpreted as a brackish, tidally influenced, middle estuarine or outer deltaic channel. This interpretation is based mainly on *Laminites*, localized lined *Skolithos* and lined *Psilonichnus* (cf. Nesbitt & Campbell, 2006). Similar *Laminites*-dominated assemblages were reported from mangrove pollen-bearing tidal channels from the Late Miocene Nauta Formation, northern Peru (Rebata *et al.*, 2006). FA1b is burrowed by a low-diversity suite of trophic generalists; this may indicate a very low salinity or freshwater setting. FA1b is interpreted as a tidally influenced deltaic channel environment.

The ichnofabric consisting of irregular burrows, shafts with bulbous enlargements and meniscate burrows, burrowing the top of FA1 (Fig. 5E and F), is interpreted as an insect-generated fabric (cf. Hasiotis, 2003). The infill of the burrows is derived from an overlying palaeosol, and therefore they most probably represent a subsequent, interchannel facies.

Facies Association 2 (localities A and C-Fig. 1)

Facies Association 2 forms sharp or gradationally based, upward-fining successions 3 m thick; it gradationally overlies FA1, or erosionally overlies similar IHS (FA2) deposits. The erosional contact is laterally limited where observable. The shape of the erosional contact can be concave-up, and it divides the deposits into imbricate cosets in places (FA2b). Upward, FA2 grades into a pedogenically altered horizon or is sharply overlain by another IHS succession. Characteristic features of FA2 are shown in Fig. 9 and include: (i) dominance of high-frequency lithological heterogeneity; (ii) cyclic rhythmites; (iii) commonness of climbing ripples; (iv) limited lateral continuity of IHS; (v) rapid changes in bedforms laterally; (vi) bigradational contacts between IHS members; (vii) limited thickness of IHS set; and (viii) lack of burrowing, or presence of fugichnia-dominated and equilibria-dominated ichnofabrics. FA2 is divided into two sub-facies associations, FA2a (Figs 7 and 10) and FA2b (Fig. 11), based on ichnological criteria (Table 2). A lithological column including FA2b is presented in Hovikoski *et al.* (2005) (location CC).

FA2: Inclined, current ripple-cross-stratified sandy silt, laminated mud and rooted mud

Sedimentological characteristics. FA2 consists of a main coarse-to-fine couplet, and of a lower frequency member. The main members are from coarse to fine: inclined, mud-draped current ripple-bearing sand and silt; and interlaminated mud and sand (Figs 10A and 11A). The thickness of the coarse member ranges from 0·5 to 8 cm. The thicker layers form flaser-bedding as cosets. The thickness of the fine member is generally 1 to 5 cm. Contacts between the members are most commonly bigradational, typically marked by mud-draped climbing ripples; as couplets, they form cyclic rhythmites. Specifically, the white noise test indicated a non-random origin for silt-clay lamina couplets ($n = 166$ couplets, $P = 0{\cdot}0001$ at FA2a; $n = 199$, $P < 0{\cdot}0001$ at FA2b). Moderately developed peaks occur at 2·4, 12, 18 and 24 couplets in the spectral density graph of FA2a (Fig. 10G). In FA2b, the peaks occur at 3·9 and 49 couplets. (Fig. 11D). The white noise test also indicates a non-random origin for the coarse-to-fine couplet cycles ($n = 31$, $P < 0{\cdot}0001$). Moderately developed peaks occur at 2 and 3·3 couplets (Fig. 10H).

Asymmetric lamina couplets are especially common in the coarse member. In addition, minor counter-current ripples, and scour-and-fill structures were observed locally. FA2b also bears synaeresis cracks and pyrite. Generally, lithology and bedforms of the members are laterally variable: the members can be followed up to a maximum of a few tens of metres. Inclination of the strata is *ca* 10° to 15°.

The lower frequency member, rooted mud, is only present in FA2a. Its thickness varies from *ca* 25 cm at the lower part of the FA (Fig. 10A), whereas at the top of the succession it is marked by a root-bearing zone of massive mud only a few centimetres thick (Fig. 10E). The vertical distance between the two rooted mud facies is 1·3 m and there are approximately 23 to 27 higher frequency, coarse-to-fine couplets between them. The lower contact of the root-bearing mud is sharp or gradational, and the upper contact is sharp and rooted; its shape is slightly concave-up and it can be followed through the whole outcrop

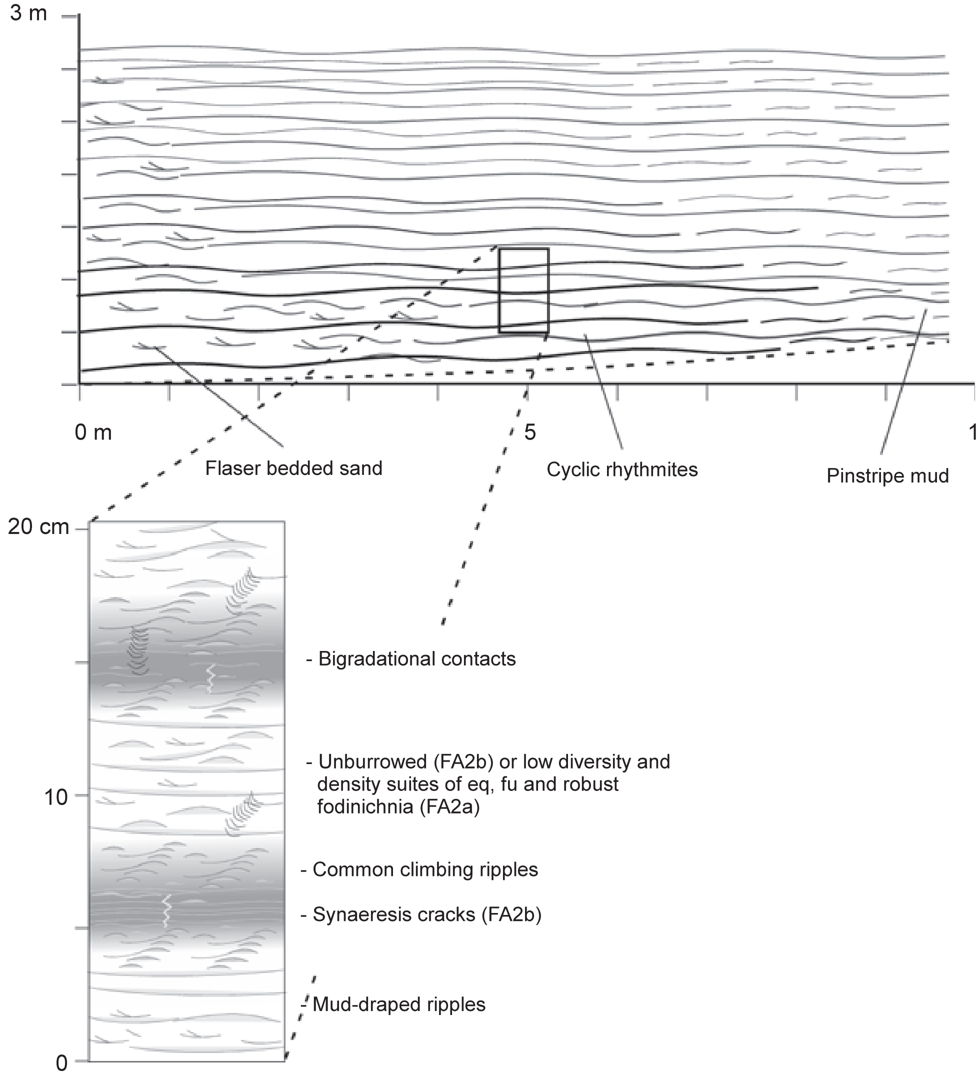

Fig. 9. Generalized schematic view of FA2. Main sedimentological and ichnological characteristics are shown.

(at least 70 m). Palaeocurrent measurements are illustrated by rose diagrams in Fig. 7.

Ichnological characteristics. The two sub-facies associations are ichnologically discrete. In FA2a, the deposits are burrowed with a low-density assemblage of vertical-to-horizontal, robust *Laminites*, vertical *Thalassinoides/Planolites*, *Palaeophycus*, and *Lockeia* that alternates with fugichnia (Fig. 10B to E). Also, *Taenidium* is present at the top of the succession. Rooted mud hosts low-diversity assemblages comprising diminutive *Planolites* and roots.

FA2b is mainly unburrowed. The only ichnofossil discovered is *Undichna* in the pinstripe mud (Fig. 11B). In addition, *Diplichnites* and *Phycodes*-like, radiating bedding plane trace fossils were observed in adjacent rhythmite facies (Fig. 11C).

Interpretation of FA2

The upward-fining grain-size and polymodal palaeocurrent directions in the IHS may suggest lateral accretion of the channel. The rhythmic sand–mud lamina couplets, their cyclic thickness variation and bipolar palaeocurrents are best explained by a tidally dominated setting. The prominent asymmetry of adjacent couplets (peak of 2·4 couplets in the spectral density diagram) and the number of couplets (up to 24) in one coarse-to-fine cycle are best explained by semi-diurnal tides (cf. de Boer *et al.*, 1989). In FA2b, the high number of couplets in a well-developed cycle (49) probably points to occasional deposition of three or four element rhythmites (Archer, 1998; cf. Hovikoski *et al.*, 2005, 2007). The inference of deposition during both flood tides and ebb tides is supported by the bipolar palaeocurrents and the cyclicity of 3·9 couplets in the

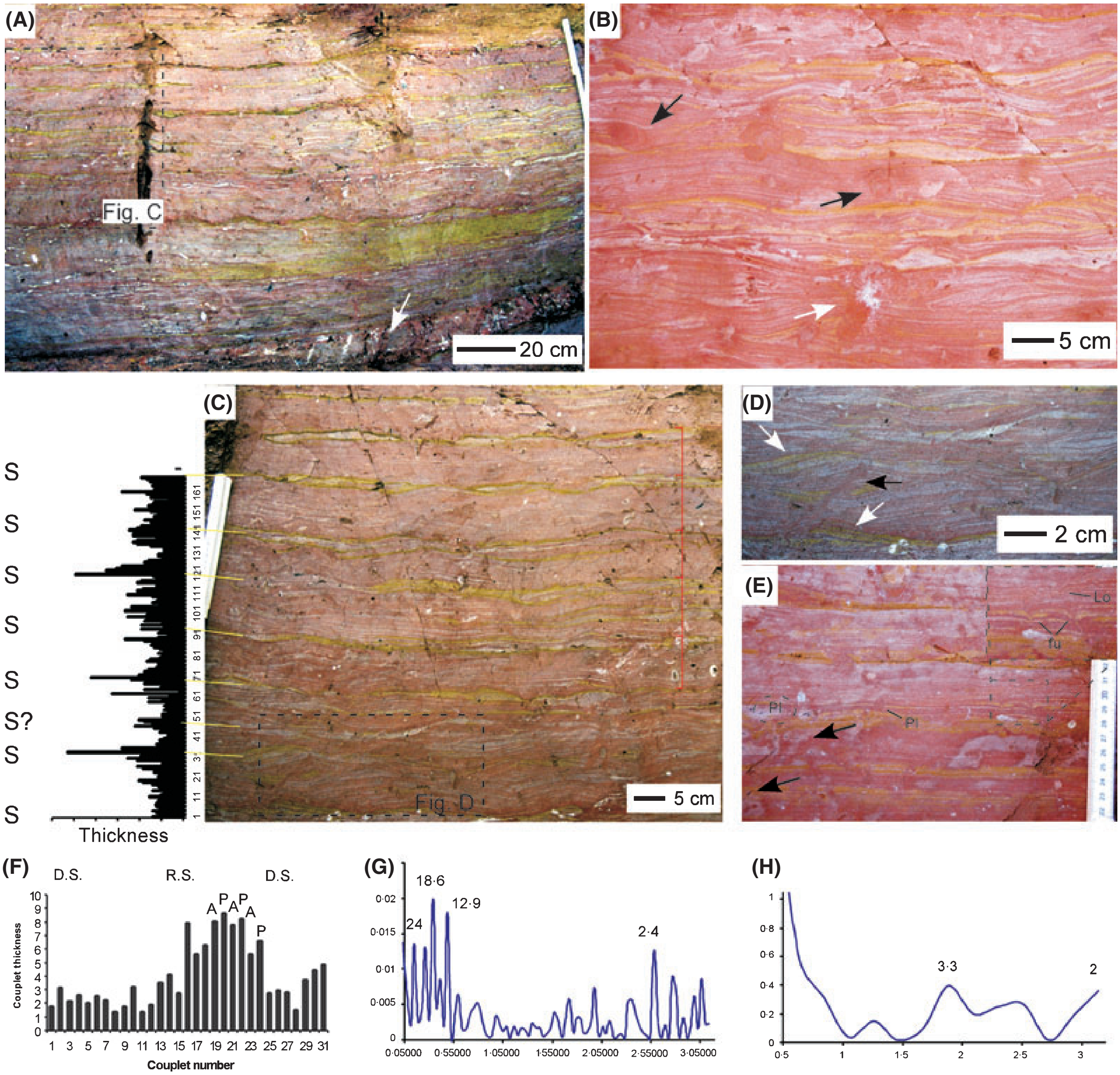

Fig. 10. (A) Overview of FA2a. White arrow indicates a root-bearing mud bed. (B) Close-up of IHS. Coarse member consists of mud-draped ripples, fine member of laminated mud. White arrow, escape/equilibrium trace; black arrows, *Laminites*. (C) IHS displaying amalgamated cyclic rhythmites. The graph shows the thickness variation of sand-clay-lamina couplets. S, interpreted occurrence of spring tides; Red bars, coarse-to-fine couplets. Fourier analysis results are shown in Fig. 10G. (D) Close-up of mud-draped ripples. White arrows, possible bipolarity; black arrow, escape trace. (E) Close-up from interval 11 to 11·5 m from the log profile. Note the increasing bed thickness above the rooted deposits. Black arrows, roots; Lo-fu, *Lockeia*-fugichnia; Pl, *Planolites*. Ruler as a scale (15 mm wide). (F) Thickness variation of coarse-to-fine couplets. Couplet 1 overlies root-bearing mud. Couplets 5 to 15 are partly truncated. D.S. and R.S., interpreted occurrence of dry and rainy seasons, respectively; A and P, interpreted occurrences of apogean and perigean spring tides, respectively. (G) Fourier analysis of lamina couplet series. Peaks occur at 2·4, 12·9, 18·6 and 24 couplets. (H) Fourier analysis of coarse-to-fine couplet (lamina bundle) series. Peaks occur at 2 and 3·3 couplets.

spectral density graph (Fig. 11D). The tidal interpretation is further supported by the commonly occurring thickness asymmetry of adjacent coarse-to-fine couplets probably indicating apogean–perigean variation (Fig. 10F).

The rooted mud facies, which is the vertically gradational equivalent of the fine member of FA1a, is interpreted as representing the lowest water levels during the year. This interpretation is supported by the number of neap–spring couplets

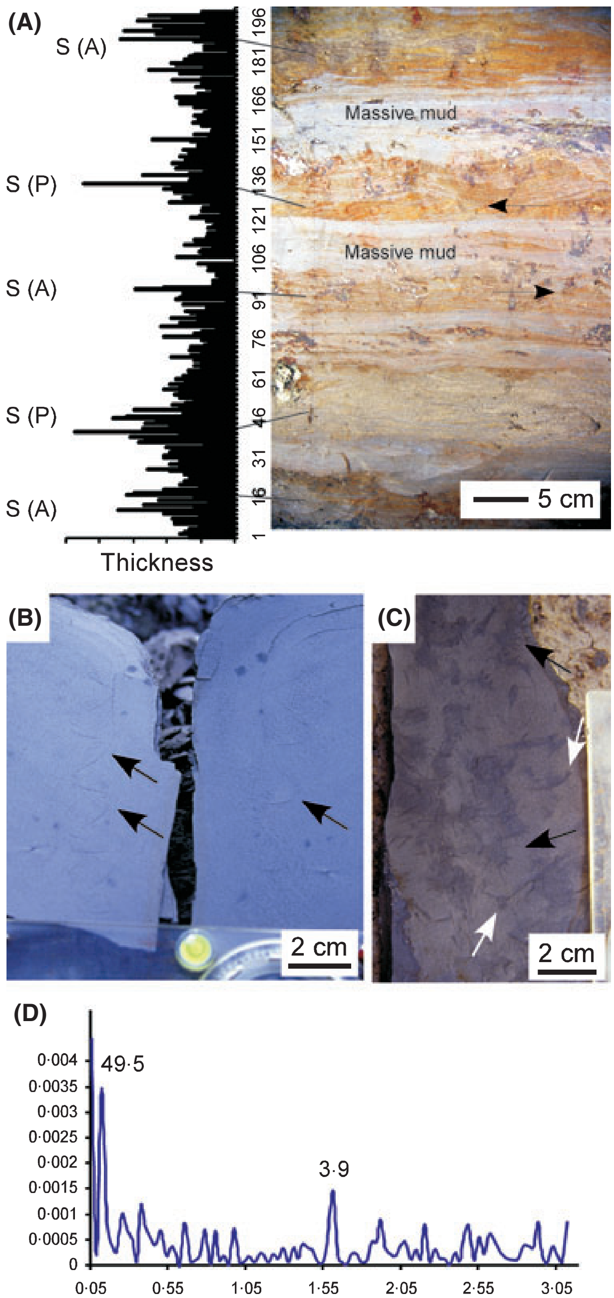

Fig. 11. (A) IHS consisting of cyclic rhythmites. The graph shows thickness variation of sand-clay-lamina couplets. Note the bipolar palaeocurrents (arrows). S(A), S(P), interpreted occurrences of apogean and perigean spring tides. The results of Fourier analysis are displayed in Fig. 11D. (B) *Undichna* in pinstripe-mud. (C) *Phycodes*-like trace fossils from adjacent rhythmite facies. White arrow, central burrow; black arrow, radiating traces. (D) Fourier analysis of lamina couplet series. Peaks occur at 3·9 and 49·5 couplets. Graph modified from Hovikoski *et al.* (2007).

(*ca* 23 to 27) between the occurrences of this facies, indicating *ca* 10 months of deposition. Moreover, the rooted mud facies is associated with decreasing bed thickness pointing to lowering accommodation space and deposition rate.

The thick–thin alternation in successive neap–spring couplets is best developed in couplets 19 to 24 (Fig. 10F), which may point to equinoctial tides. This interpretation is based on the modern seasonality in the region (discussed below): the dry season begins on average in May (couplets 23 to 28); whereas, the equinoctial maxima in tides occur in late March (couplets 19 to 24). Autumnal equinoctial maxima occur in late September that would operate concurrently with the next rainy season (couplets 1 to 5). In the latter case, the possibly occurring asymmetry is more subjective due to truncated couplets.

In FA2b, the lack of bioturbation is probably mainly due to physical stress such as high aggradation rates (fortnightly up to 13 cm), fluctuating salinities (see below) and turbidity stress, as indicated by the common presence of mud-draped climbing ripples. The channel successions observed in outcrop are not capped by pedogenic horizons, which suggest permanently sub-aqueous deposition, probably in a sub-tidal deltaic bay setting.

The *Laminites*-dominated ichnofabric of the FA2a implies saline bottom waters. There are no clear salinity indicators in FA2b, but the presence of synaeresis cracks may indicate fluctuating salinity. Also pyrite may point to some saltwater influence in the facies. FA2b is interpreted as subtidal creek in a deltaic bay. In summary, the FA1a to FA2a gradation represents a change from a high-energy, low-salinity/freshwater, tidally influenced and seasonally controlled setting to a tidally dominated, saline, low-energy, combined suspension and traction-driven environment. This result probably implies an abandoned deltaic channel infilled with lower energy estuarine deposits (cf. Dalrymple *et al.*, 2003).

Facies Association 3 (localities D, E and F-Fig. 1)

FA3 forms sharp-based, upward-fining successions up to 8 m high; they are capped by the same FA, a pedogenic horizon, or a muddy, sharp-based, desiccation crack-bearing upward-fining succession. Characteristic features of FA3 are shown in Fig. 12 and include: (i) dominance of low-energy bedforms (current ripples); (ii) moderately thick, IHS successions and couplets; (iii) laterally extensive IHS members; (iv) rhythmic occurrence of low-frequency IHS; (v) imbricate cosets; and (vi) localized presence of freshwater fossils. An articulated, side-necked turtle fossil

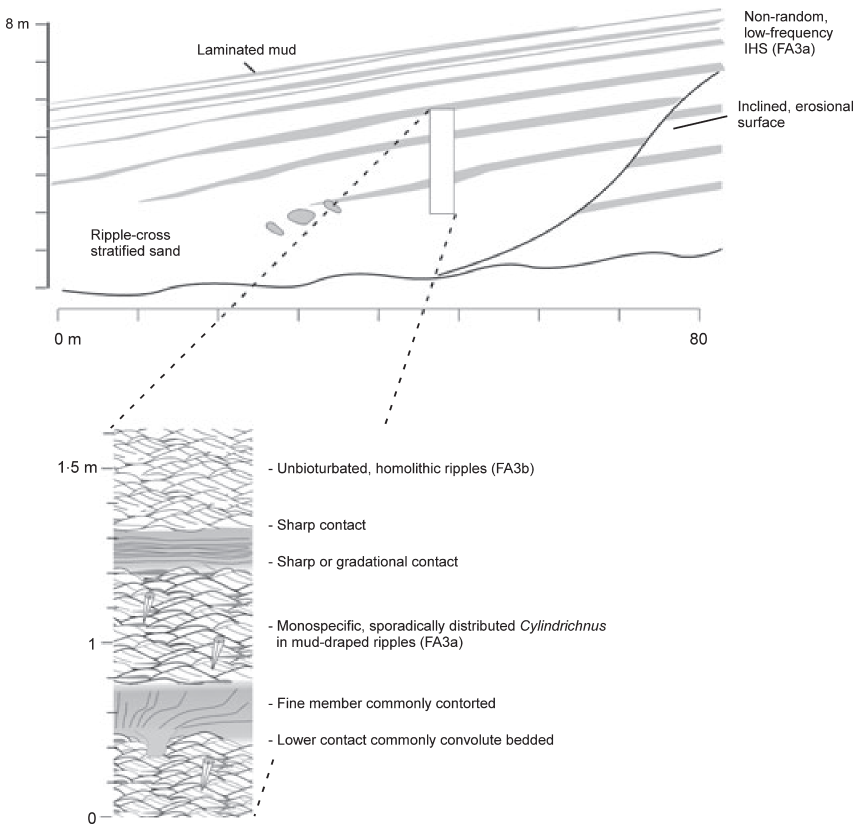

Fig. 12. Generalized schematic view of FA3. Main sedimentological and ichnological characteristics are shown.

has been discovered from the facies association at locality D (Carvalho *et al.*, 2002). FA3 is divided into two sub-facies associations, FA3a (Fig. 13A and B) and FA3b (Fig. 13C and D), based on lithological and ichnological criteria (Table 3). Localities D and E were described earlier in Räsänen *et al.* (1995).

FA3: Inclined, ripple-cross-stratified fine-grained sand (A) and massive or laminated mud (B)

Sedimentological characteristics. Facies Association 3 consists of a coarse-to-fine couplet. The members are: (A) inclined, ripple cross-stratified fine-grained sand; and (B) inclined, massive or laminated clayey mud (Fig. 13A and B). In the lower part of the successions, the coarse member bears small-scale trough cross-stratification in places, and forms a minor IS-set. The coarse member can be mud draped (FA3a) or homolithic (FA3b) (Fig. 13B and C); its thickness ranges from a few centimetres to 2 m. The contact from fine to coarse is sharp, but commonly bears deformation structures (convolution, loading). Deformation increases in the down-dip direction where the beds can be fully contorted. The contact from coarse to fine ranges from gradational to abrupt. The thickness of the fine member ranges from a few centimetres to 30 cm. The couplets are generally from 10 to 230 cm thick. Commonly, adjacent couplets are strongly asymmetric (Fig. 13D). Lateral continuity of the couplets is limited by inclined erosional contacts that divide the beds into imbricate cosets, but the beds can be followed up to at least 60 m. True dip of the beds is about 15° to 20°. The angle tends to flatten out in an up-dip direction.

The IHS couplets may form either random or cyclic series. In particular, the white noise test indicates a non-random origin for one FA3a IHS succession (lateral series, $n = 111$, $P < 0{\cdot}0001$). Peaks occur at 4·4, 5, 10 and 22 couplets in the spectral density plot (Fig. 13E). One brief FA3b IHS succession turned out to be random ($n = 21$). Palaeocurrent measurements are illustrated by rose diagrams in Fig. 11A.

Ichnological characteristics. Low-density assemblage consisting of rare, small-to-moderate *Planolites*, *Skolithos*, *Arenicolites* and meniscate burrows lace the facies association. In addition, sporadically distributed *Cylindrichnus* occur in mud-draped cross-strata of FA3a (Fig. 13B).

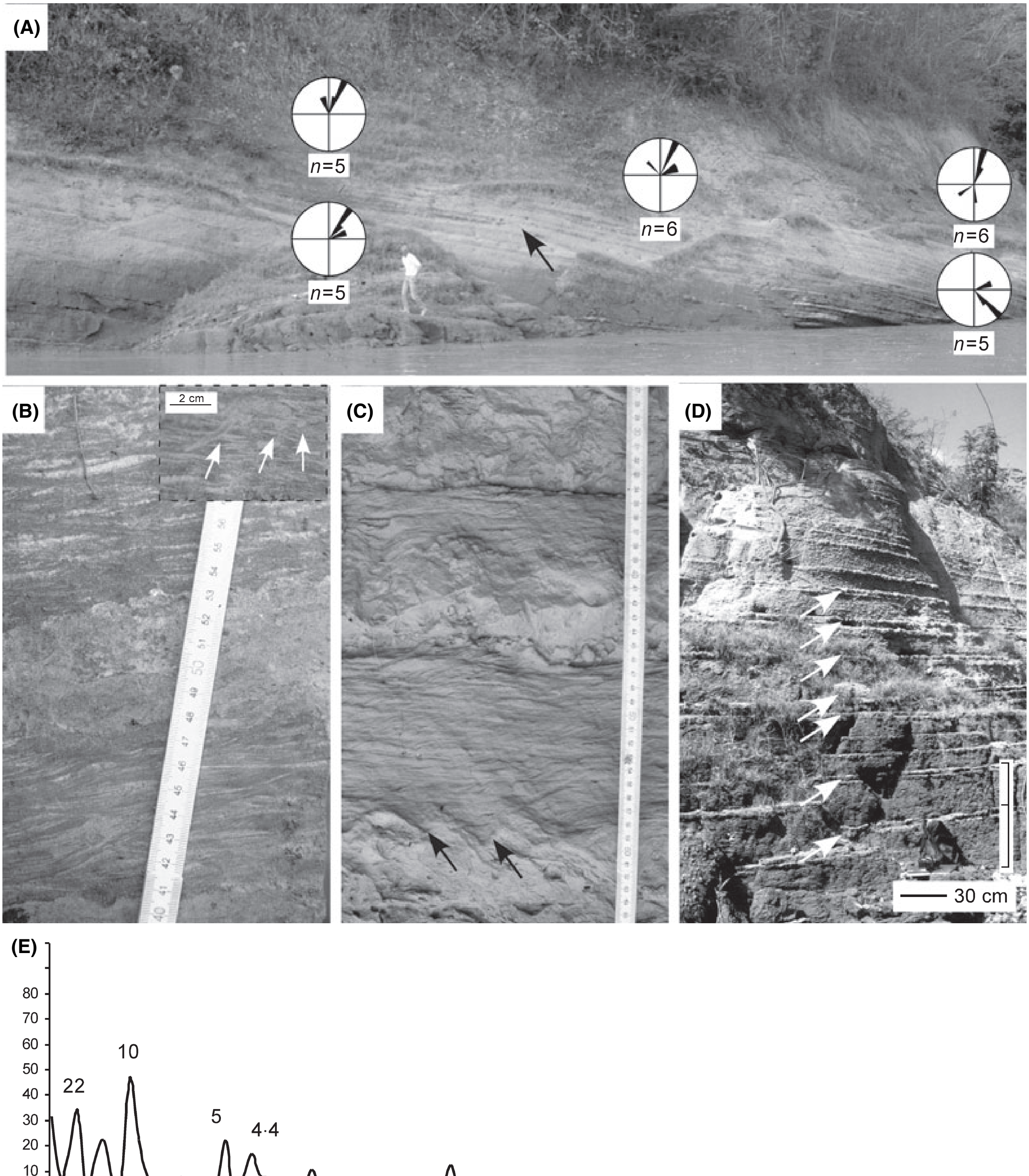

Fig. 13. (A) A photograph of location D. Black arrow, inclined erosional contact. Person as a scale (*ca* 1·8 m tall). (B) IHS consisting of mud-draped, ripple-cross-stratified sand and massive mud at location E (FA3a). The close-up photo shows *Cylindrichnus* (white arrows). Ruler as a scale (15 mm wide). (C) IHS consisting of ripple-cross-stratified sand and massive or laminated mud at location D (FA3b). Black arrows, convolute bedding. Ruler as a scale (15 mm wide). (D) IHS consisting of ripple cross-stratified sand and massive or laminated mud at location F (FA3b). White arrows, asymmetric couplets; black bars, composite couplets used in spectra analysis. (E) Fourier analysis of FA3a IHS. Peaks occur at 4·4, 5, 10 and 22 couplets.

Interpretation of FA3

The upward-fining succession with a truncated, sharp base is best explained by a channel environment. In addition to the general upward fining character of the succession, the palaeocurrent directions change upward within the set (Fig. 11A) pointing to the meandering nature of the channel. The couplet thickness (up to 230 cm) and lack of evidence of tidal dominance in FA3 point to annual cyclicity. The great number of mud-draped strata in couplets of FA3b support this interpretation and imply a superimposed tidal influence. The low-frequency cycles of 4·4, 5, 10 and 22 couplets (years) may be related to El Niño periodicity but more data are needed to allow a more reliable interpretation. The repeatedly occurring, prominent thick–thin alternation in successive couplets up to 2 m thick (Fig. 11D) is probably due to equinoctial (i.e. zenithal) rains that may cause two distinct annual rainy seasons of different magnitudes close to the equator (e.g. McGregor & Nieuwolt, 1998). The asymmetry of successive rainy seasons increases with increasing distance from the equator, reaching a maxima around latitude 10° in an ideal case. Further away from the equator (around latitude 15°), the two rainy seasons merge into one. The phenomenon of a double rainy season occurs in Amazonia presently, but it is not developed in Acre today.

The freshwater turtle fossil discovered from FA3b was articulated and, considering the low-energy bedforms, was probably deposited *in situ*. The ichnofabrics, especially the patchy monospecific suites of *Cylindrichnus,* suggest sporadic brackish-water influence at least in the most tidally influenced facies (FA3a). In concert, the above-mentioned sedimentological, ichnological and palaeontological data most probably point to a seasonally controlled, fluvio-tidal point bar.

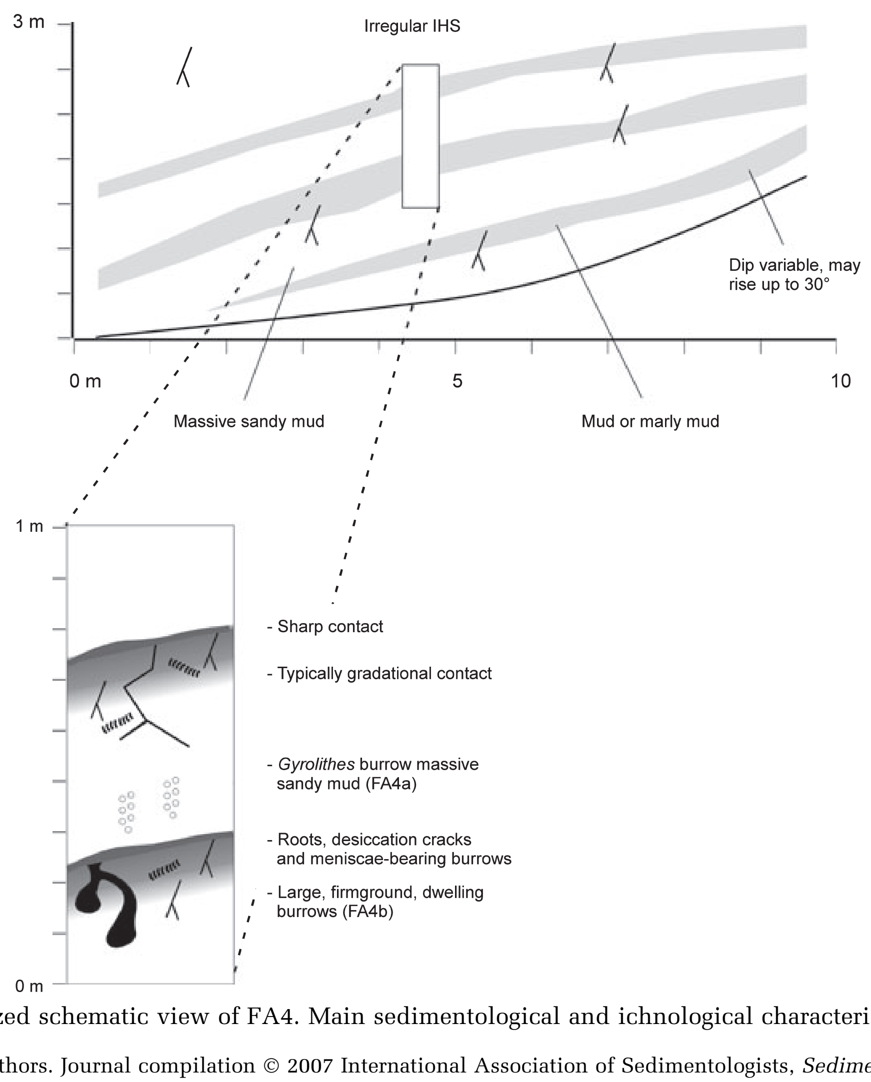

Fig. 14. Generalized schematic view of FA4. Main sedimentological and ichnological characteristics are shown.

Facies Association 4 (localities A, B, G and H-Fig. 1)

FA4 forms 2 to 4 m thick, upward-fining successions (Figs 6 and 7); its lower contact is sharp where observable. The geometry of the contact is variable, ranging from a laterally limited, strongly concave-up to a laterally extensive, flat surface. Typically, FA4 grades upward into a pedogenically altered horizon, or is erosionally truncated by another IHS succession at its top. Characteristic features of FA4 are shown in Fig. 14 and include: (i) relatively thin IHS successions; (ii) lack of an IS-set; (iii) lack of higher frequency lithological heterogeneities; (iv) laterally limited, irregularly occurring IHS; (v) massive appearance of members; (vi) roots, desiccation cracks or firm-ground burrows bearing fine members; (vii) organic-rich or marly matrix; and (viii) localized presence of freshwater fossils. FA4 is divided into four sub-facies associations, FA4a (Fig. 15A to C) and FA4b to FA4d (Fig. 15D to G), based on lithological and ichnological properties (Table 4). An articulated Purussaurus-fossil (a freshwater alligator) was discovered from FA4c.

FA4: Inclined, massive or stratified sandy mud (A) and inclined, root-bearing mud (B)

Sedimentological characteristics. FA4 consists of a coarse-to-fine couplet. The members are inclined, 20 to 60 cm thick, massive or stratified, sandy mud or muddy sand, and irregular, root-bearing mud (Fig. 15A). Rarely, laminations (FA4d) and trough cross-stratification is observed in the coarse member (FA4b). Otherwise, the coarse member has a massive appearance. The matrix commonly displays a dark, brownish colour. The fine member also has a massive appearance, commonly bears roots and/or desiccation cracks, and is 5 to 15 cm thick; typically, it consists of marly mud (Fig. 15D). The contact from coarse to fine is usually irregular and sharp, even though the change in grain-size is somewhat gradational. The contact from fine-to-coarse couplets is sharp.

Typically, FA4 IHS beds are laterally limited and can be followed from a few metres to a few tens of metres. IHS interbedding is irregular. The dip is variable, but was typically 15° to 20°. Furthermore, FA4 contains minor faults up to 20 cm deep.

Ichnological characteristics. Most commonly, the coarse member is unbioturbated, or yields burrows that descended from the fine member. In places, however, suites consisting of *Palaeophycus* and *Gyrolithes* (FA4a; Fig. 15B) or *Planolites* are observed. The bioturbation degree is generally low (<10%), but may reach up to 50% in some beds. Locally, roots, *Taenidium* (Fig. 15C), large and deeply penetrating branching burrows (Figs 14F and 15E), and simple, I-shaped *Psilonichnus* descend from the fine member. The two latter mentioned biogenic structures are unlined and passively filled by marly matrix. In places, the roots are completely reburrowed by small *Planolites*. The top of the FA is typically burrowed by *Taenidium*. The bioturbation intensity of this suite also remains low (less than 10%).

Interpretation of FA4

The truncated lower contact and upward-fining grain-size point to a channel environment. The deep desiccation cracks (Fig. 15G) and roots suggest regularly occurring sub-aerial exposure. The passive infill of unlined burrows descending from the fine member in places indicates a consolidated substrate. Considering abundant roots and pedogenic features, and no signs of erosion, the compaction is most probably due to sub-aerial dewatering. The rooted deposits and the associated complex, permanent dwelling burrows point to longer time cycles than seven days for the fine member development. Consequently, the fine member is interpreted as having formed during dry seasonal sub-aerial exposure of a channel, rather than during its active lateral accretion. The seasonal cyclicity is also supported by the thickness of the IHS couplet (up to 50 cm), and the lack of tidal indicators.

The presence of an articulated freshwater alligator fossil find, and ichnofabrics consisting of *Taenidium* with common root bioturbation, point to a continental affinity. However, the observed *Gyrolithes–Palaeophycus* intervals probably indicate a fluctuating, very low salinity (possibly oligohaline) setting for FA4a. A very similar assemblage is documented from modern and Pleistocene tidal creek point bar deposits in the Willapa Bay estuary, USA (Gingras *et al.*, 1999).

DISCUSSION

The deposits taken together represent tidally and seasonally influenced, laterally accreting channel complexes that are intercalated with pedogenic horizons, fluvial channels and sub-tidal shoal deposits.

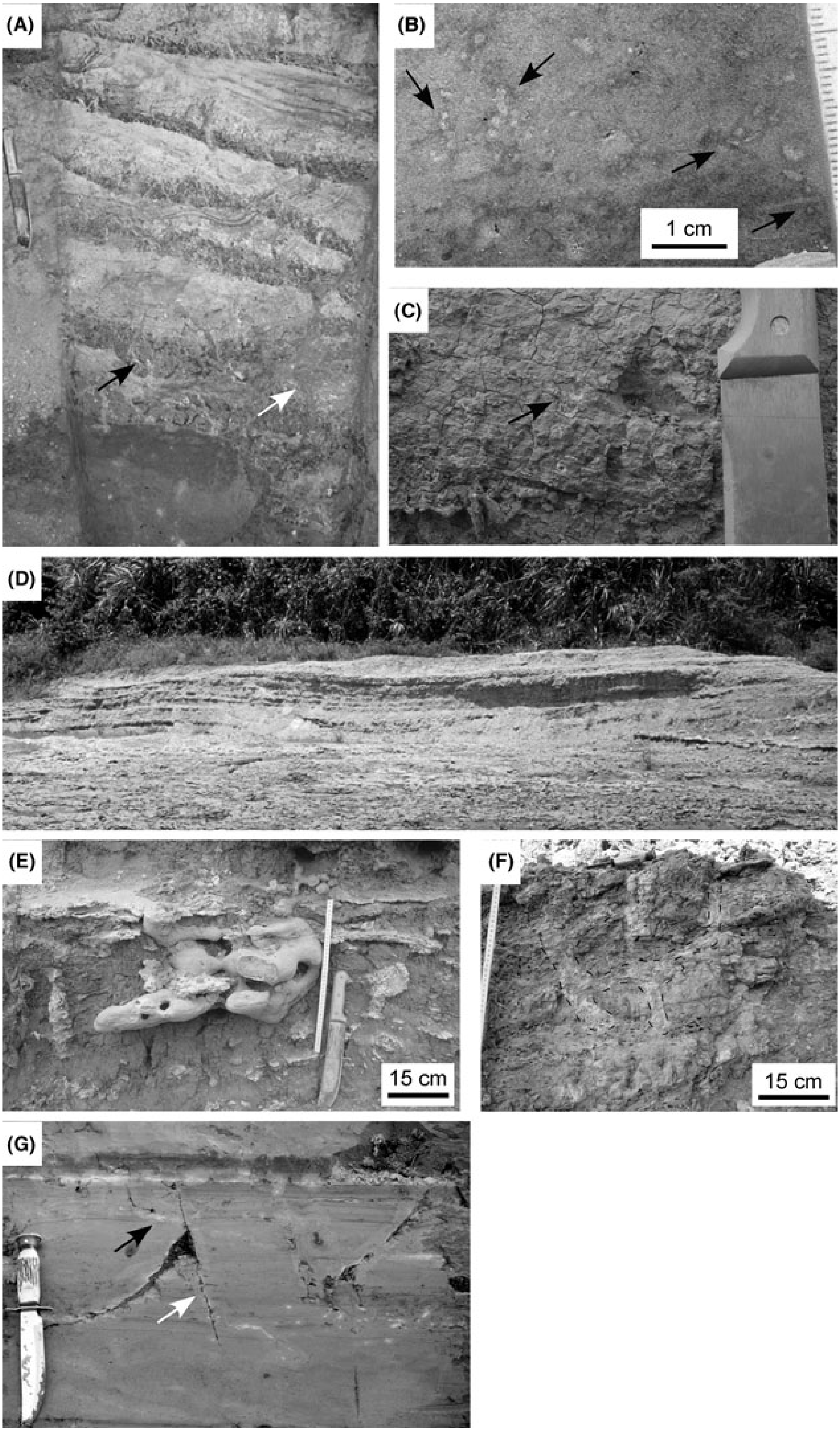
(A)
(B)
1 cm
(C)
(D)
(E)
15 cm
(F)
15 cm
(G)

Depositional environments

The pedogenic horizons may be well-developed (palaeosoils) or comprise immature horizons with unionid bivalves (freshwater flood plains). The deposits represent mainly low-saline to freshwater conditions, but also periodically mesohaline settings (as reflected by *Laminites*-lined *Skolithos*-lined *Psilonichnus* ichnofabrics). Above, the deposits were divided into four, broad channel-fill types primarily based on sedimentological criteria. Although a great deal of the sedimentological variability was not strictly salinity dependent, Facies Associations 1 and 2 generally represent more distal parts of the depositional system, whereas Facies Associations 3 and 4 represent more proximal positions. This division is generally supported by channel sizes that are the largest in the examples interpreted as most distal, excluding minor tidal creeks and abandoned tidal channels not attached to the fluvial system. In addition, the flow velocities were usually the highest in the distal examples. In the following text, the variability of temporal controls in relation to the position of the saltwater wedge is considered more closely. For this purpose, the sub-facies associations are divided into three facies belts: distal, middle and proximal (Fig. 16).

Distal setting: brackish, tidally dominated or influenced channels (FA1a and FA2a)

These deposits contain evidence of superimposed annual and tidal influence. Time-series analysis indicated the presence of cyclic tidal rhythmites in low-energy settings in this facies belt. The recognizable neap–spring–neap cycles reach 8 cm thickness at a maximum (Fig. 5C), whereas the annual depositional rate produced up to 1·3 m thick deposits in an upper point bar setting (FA1a). Both FA1a and FA2a stratigraphically overlie more restricted channels, which indicate either transgression or autocyclic changes. If the sediments were transgressive, they would be best explained by mesotidal (see below), middle estuarine point bars (in the sense of Dalrymple *et al.*,

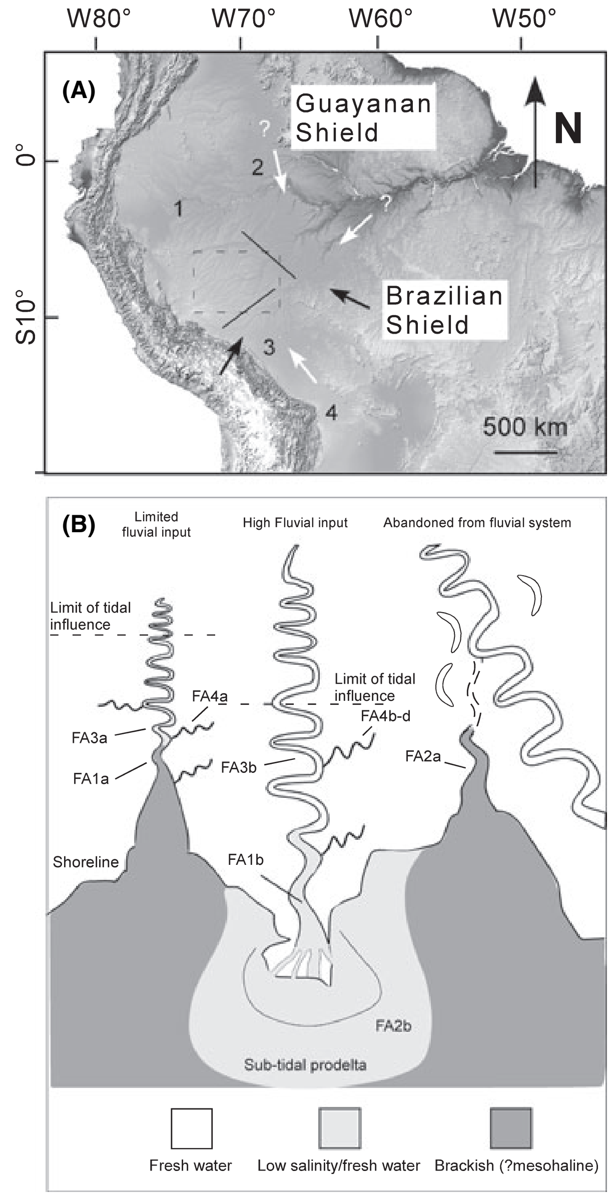

Fig. 16. (A) Map of western Amazonia displaying potential directions for marine influence (white arrows; Hovikoski *et al.*, 2007) and sediment sources (black arrows; Roddaz *et al.*, 2006). The numbers indicate other reported Late Miocene epeiric deposits: (1) Nauta Fm. (Rebata *et al.*, 2006), (2) Apaporis sand unit (Hoorn, 2006), (3) Beni sub-basin (Roddaz *et al.*, 2006), (4) Yecua Fm. (Hernández *et al.*, 2005). (B) Generalized schematic interpretation of the depositional system.

Fig. 15. (A) Interbedded, massive sandy mud and rooted mud (FA4a). Black arrow, roots; white arrow, crack. Knife as a scale (*ca* 40 cm long). (B) Close-up of *Gyrolithes*, *Palaeophycus* ichnofabric. Black arrow, *Gyrolithes*. (C) *Taenidium* from the top of the succession. (D) Interbedded inclined bioturbated sandy mud and marly mud beds at location G (FA4b). The outcrop is *ca* 30 m wide. (E) and (F) Close-up of a large, passively filled burrow descending from fine member. (G) A close-up of FA4d. The normally graded couplet consists of massive muddy sand and desiccation crack bearing mud. White arrow, desiccation crack; black arrow, burrow mottling. Knife as a scale (*ca* 20 cm long).

1992). Alternatively, the FA1b to FA2a gradation may represent a deltaic setting that became more tidally dominated after abandonment of the fluvial system (cf. Dalrymple *et al.*, 2003; see also Van den Berg, 1981; Rebata *et al.*, 2006).

Middle setting: low and/or fluctuating salinity, with tidal or annual control (FA1b, FA2b, FA3a and FA4a)

These deposits show evidence of low and/or fluctuating salinities such as *Gyrolithes* or low-diversity assemblages of trophic generalist-dominated ichnofabrics (FA1b, FA4a), monospecific suites of *Cylindrichnus* (FA3a), or sedimentological properties perhaps related to a saltwater influence (synaeresis cracks, pyrite) (FA2b). Sedimentologically, the deposits typically contain cyclic tidal rhythmites or clear, superimposed tidal and seasonal cycles. In addition, time-series analysis indicated non-random origin for a seasonal IHS succession in this facies belt (FA3a). The yearly depositional rates reached over 2 m in large, sub-tidally influenced channels (FA1b); whereas, in smaller tidal channels, annual vertical accretion was up to 30 to 50 cm (FA4a). Cyclic tidal rhythmites in FA2b suggest that tidal amplification reached the limit of the saltwater wedge.

Proximal setting: freshwatered IHS channels with annual control (FA3b and FA4b,c,d)

Continental ichnofabrics and articulated freshwater fossils support the interpretation of a predominantly freshwater origin. Characteristically, the channelized fine members consist of muddy or marly beds that commonly contain evidence of sub-aerial exposure (desiccation cracks, roots). The deposits typically are dark brownish in colour, probably indicating that originally the strata bore organic matter concentrations. Strong asymmetry in adjacent couplets formed in continuously sub-aqueous riverine channels (FA3b). The yearly depositional rate was 10 to 230 cm in the reported examples. Moreover, these deposits do not generally yield evidence of a clear tidal influence such as rhythmic, higher frequency lithological heterogeneity in IHS. Also, time-series analysis for a brief, seasonal IHS succession indicated a random origin (FA3b) in this facies belt. However, none of the reported IHS channels are associated with crevasse-splay deposits, possibly indicating that the channel dynamics were not entirely fluvially driven, even in the most proximal IHS setting (Barwish, 1978). The formation of sub-aerially exposed fine members probably corresponds to a passive phase rather than active lateral accretion of a channel. The facies belt probably represents an inner estuarine or proximal delta-plain setting, close to the limit of tidal influence.

The depositional system

The number of couplets in one neap–spring cycle and the pronounced diurnal inequality most probably indicate a mixed or semi-diurnal regime for Acre. The centimetre-scale, cyclic tidal rhythmites (FA2), tidal creek facies associations, and the tidally influenced UFR deposits (FA1b) point to a somewhat elevated tidal range (Archer, 1998; Kvale & Mastalerz, 1998). The biogenic properties of the tidal facies, the dominance of tidal channel facies in the regional sedimentary record, and the restriction of tidal rhythmites to channels are more consistent with mesotidal than macrotidal conditions. Also generally in upper Amazonian basin deposits, the rhythmites described are reported from channels or large burrow infills (tubular tidalites), where the topographic setting provided the accommodation space (Räsänen *et al.*, 1998; Gingras *et al.*, 2002; Hovikoski *et al.*, 2005). Finally, the preservation of almost complete tidal rhythmite successions may suggest relatively weak tidal currents in a shallow water setting (Wells *et al.*, 2005).

The annual cyclicity observed in every part of the depositional system is most probably due to migration of the Inter Tropical Convergence Zone (ITCZ) that causes strong seasonal changes in precipitation. Today, from June to August, precipitation is low, while in December to April rainfall can rise to close to 300 mm in a month. An average yearly rainfall is about 2000 mm. A similar migration of the ITCZ and rainfall intensity was already present in upper Amazonia during the Miocene, based on oxygen isotope variations in incremental growth bands of fossil bivalves (Kaandorp *et al.*, 2005). At present, the strong seasonality considerably affects water levels, and the river water table may drop by as much as 8 m in Acre during the dry season (Archer, 2005).

Another important controlling factor was the slope of the depositional system. The slope in the area is low today. The altitude of Iquitos (Peru) is around 114 m above sea-level; it is situated 2975 km inland from the Amazon River mouth (i.e. a change in altitude of 3·8 cm per kilometre) (Archer, 2005). It is reasonable to assume that, during the time of deposition, the slope was even lower, because accelerated tectonic subsidence took place in the western Amazonian foreland basin in the Middle to Late Miocene (Hermoza, 2004). In addition, global sea-level was probably higher then than it is today, presuming that deposition was not coincident with the Late Miocene sea-level drops. Finally, the present-day altitude of the Iquitos area is affected by post-Miocene deformation and by the rise of structural arches due to an eastward migrating forebulge (Roddaz *et al.*, 2005a,b).

The inferred extremely low relief allowed rapid progradation and retrogradation of the shoreline, and probably controlled the lateral accretion of the channels. Consequently, this situation explains the close spatial and temporal occurrence of terrestrial and marginal marine strata in the sedimentary record. Even though correlation between individual outcrops is not possible, the wide distribution of IHS channels in every part of the Acre sub-basin probably indicates persistent, or repeated, marginal marine influence in the area. In addition, marginal marine/tidally influenced deposits are reported from presumably contemporaneous strata in other western Amazonian foreland sub-basins (Pastaza-Marañon: Rebata *et al.*, 2006; Madre de Dios: Hovikoski *et al.*, 2005; Chaco: Hernández *et al.*, 2005; Beni: Roddaz *et al.*, 2006) indicating that the Late Miocene ingression covered much of the interior of the continent. The dominance of terrestrial fossils in the Acre sub-basin (e.g. Latrubesse *et al.*, 1997) probably indicates that the marginal marine episodes represent briefer time cycles and/or had spatially narrower occurrences than the intercalated continental strata.

The applicable analogies to the depositional system are estuarine and delta-related systems such as the modern Amazon and Fly River deltas (Archer *et al.*, 2005; Dalrymple *et al.*, 2003 respectively). Both examples have strong tidal and seasonal controls in deposition within a low relief setting.

Interpreted annual and neap–spring signatures in IHS

In the text below, the sedimentological and ichnological responses to different temporal controls are compared, these are summarized in Table 5.

Contacts and shape of IHS couplets

The contacts of neap–spring-generated couplets are most commonly bigradational in the Acre sub-basin; thus, their appearance is diffuse. In some cases, erosion is involved in the lower contact of the coarse member. However, even in these cases a couplet typically consists of flaser-lenticular bedding and the change from fine-to-coarse member is partly gradational. The gradation from coarse-to-fine members most commonly constitutes mud-draped, climbing ripple structures in the best developed cyclic rhythmites.

The contacts of seasonal couplets are gradational or sharp from coarse to fine and abrupt from fine to coarse in Acre. The comparable trend is observed also in several other similarly interpreted couplets (e.g. Van den Berg, 1981; Smith, 1988; Bechtel *et al.*, 1994). Despite the common normal grading from coarse to fine, both members are most often distinct. As a result, the couplets are generally more tabular and bed-like than the fortnightly ones. The dry seasonal members may turn to more concave-up and reach considerable dips, especially in the proximal part of the system. The tidally dominated IHS tends to show lower inclinations.

Lateral continuity and variability of IHS couplets

The neap–spring couplets can be followed laterally only in part of the channel-body, a few tens of metres at maximum. The lithology and bedforms of these couplets may change rapidly: the flaser-wavy-bedded neap–spring couplets in Fig. 11 change to massive/pinstripe mud over a few metres distance in sub-tidal creek deposits. The same trend is observed in other similarly interpreted sediments (e.g. Greb & Archer, 1998).

The seasonal couplets can be traceable through most of the channel-body, typically up to 100 m, depending on the preservation (cf. Van den Berg, 1981; Ainsworth & Walker, 1994). In small tidal creeks the lateral continuity is more limited. The difference in height between the down-dip end and the up-dip end can reach at least 3 to 5 m (FA1, FA3). In terms of lithology and bedforms, the members are more uniform although they become finer-grained up-dip (Siiro *et al.*, 2005). A comparable trend is reported in other similarly interpreted deposits (Mossop, 1975). Seasonal fine members commonly form intraformational breccias in rapidly aggrading tidally influenced settings.

Rhythmicity of IHS couplets

Neap–spring cycles of IHS appear rhythmical and display cyclic rhythmites in the reported examples; in spectral analysis, they show cyclicities

Table 5. Summary of interpreted annual and neap–spring signatures in IHS in Acre.

Property	Annual	Neap–spring
(1) Thickness of IHS members	Coarse member: 5 cm to 2 m. Fine member: 5 to 60 cm. Couplet: 10 cm to 2·3 m	Coarse member 1 to 8 cm. Fine member 1 to 5 cm. Couplet 2 to 13 cm
(2) Thickness variation within an IHS set	Member: 10 cm to 2 m. Couplet: from 20 cm to 2 m	Member 4 to 8 cm. Couplet from 2 to 8 cm
(3) Contacts of IHS members	From coarse to fine gradational or sharp. From fine to coarse: sharp, often bear evidence of sub-aerial exposure, sub-aqueous truncation or deformation	Contacts often bigradational, sometimes base of the coarse member shows evidence of erosion
(4) Shape of IHS members	Tabular, 'bed like'	Tabular, diffuse
(5) Thickness of adjacent IHS members	Asymmetric in places*	Often asymmetric
(6) Lateral continuity of IHS	Traceable through most of the channel-body, up to 100 m. In small tidal creeks lateral continuity is more limited. Lithology and bedforms fairly uniform. Up to 3 to 5 m vertical extent between up-dip and down-dip ends	Traceable few tens of metres in maximum. Lithology and bedforms may change in few metres distance
(7) Inner structures in IHS members	Coarse member: cross-stratified or massive. Fine member: massive or laminated, often bears faults, roots and desiccation cracks, may get brecciated and/or contorted down-dip	Coarse member: mud-draped ripples, flaser-bedding. Fine member: often climbing rippled heterolithic mud, massive or laminated
(8) Cyclicity of IHS couplet series	Random or non-random. Cycles of 4·4, 5,10 and 22 couplets	Non-random. Cycles attributable to daily, fortnightly and monthly cycles in 2 to 4 element rhythmites
(9) Ichnological variability in IHS	Genus-level changes in adjacent members. Change in trace fossil behaviour in adjacent members. Bioturbation often concentrated in one of the members. Compound ichnofabric in couplets <50 cm thick. High-density assemblages in couplets <50 cm thick. Also permanent, robust dwelling and feeding burrows. Occasional firm-ground assemblages in sub-aerially exposed beds	Minor or no genus-level changes between members. Minor change in bioturbation intensity in adjacent members. Low-density, simple tier assemblages in couplets >2 cm thick. Fugichnia and fodinchnia by mobile deposit feeders dominate in couplets >2 cm thick. Moderate density compound assemblages in couplets <2 cm thick. No bioturbation in stressed settings

Table 5. (*Continued*)

Property	Annual	Neap–spring
(10) Interpreted process	Coarse member: active lateral accretion. Fine member: active, occasionally passive	Both members: active lateral accretion
(11) Interpreted relationship to saltwater wedge	Occurs on both sides of saltwater wedge	Not recognized in permanently freshwater setting

*May be limited to near equatorial settings.

that can be realistically related to semi-diurnal and neap–spring processes (Figs 10G and 11D), even though the series analysed were not perfectly developed. Additionally, neap–spring couplet series produced non-random successions locally (Fig. 10F). The spectral density peaks can be reasonably interpreted as being due to an apogean–perigean variation (Fig. 10H). Furthermore, the thickness variation of fortnightly couplets is only a few centimetres within a set. By contrast, the seasonal IHS couplets may display considerable thickness variation within a set (e.g. minimum 15 cm, maximum 70 cm, FA3) and reach more than 2 m in thickness. However, even seasonal interbedding can produce non-random heterolithic series in deposits that bear well-defined superimposed tidal influence (Fig. 13E). Whether the low-frequency cyclicities observed were due to El Niño or other phenomena will be a subject of further research. Finally, the thick–thin alternation of successive couplets can occur repeatedly in seasonal beds as well (Fig. 13D, see FA3 for discussion). This phenomenon may be restricted to tropical equatorial settings.

Ichnological variability in IHS

No distinct ichnogenera-level changes occur in adjacent neap and spring members. Both members consist generally of a non-composite, low-density and low-diversity fabric in 2 to 8 cm-thick couplets for the most distal setting. The infaunal trace fossils (e.g. *Laminites, Thalassinoides* and *Planolites*) commonly display robust fodinichnia, equilibrichnial or fugichnial behaviours in these brackish-water deposits (Fig. 10A and D). Generally, bioturbation intensity is low in coarse (0% to 10%) and fine (5% to 30%) members. Bioturbation intensities can rise to 60% to 80% when the fortnightly depositional rate drops to 1 to 2 cm. In this case, the ichnofabric is dominated by mobile deposit feeders and localized fugichnia of small-sized organisms (Fig. 10E). In cases of fluctuating salinity and high water turbidity, bioturbation is generally absent except for the sporadic occurrence of bedding plane-confined traces (FA2b).

All the bioturbated seasonal examples show considerable ichnogenera-level changes between members at Acre (cf. Lettley, 2004). In particular, in the proximal examples where the fine members are associated with sub-aerial exposure, the change is apparent (Fig. 15E and F). Firm-ground assemblages developed periodically in these beds. Furthermore, fine members show permanent dwelling and feeding burrows where they represent prolonged pause planes (e.g. Fig. 15E). High-density composite fabrics can occur in couplets as thick as 50 cm. In energetic, tidally influenced, rapidly aggrading channels (1 to 2·5 m annually), the infaunal community displays a simple tiered structure where shallow tier traces were concentrated on the mud-draped strata. Bioturbation is typically concentrated in one of the members. The coarse-grained member is commonly more bioturbated than the fine member in fluctuating/low-salinity and freshwater settings (FA1b, FA4a); this probably is due to increased turbidity stress during the dry season in these proximal locales (landward migration of turbidity maxima). Fine-grained members yield more intense bioturbation in distal positions (FA1a).

CONCLUSIONS

A detailed ichnological, sedimentological and statistical study of upper Miocene strata of the Solimões Formation leads to the following conclusions:

1 The deposits studied can be divided into four broad channel-fill types and several sub-associations; they represent various types of inclined heterolithic stratification deposits that are mainly capped by pedogenic horizons. The strata are interpreted as estuarine-related or delta-related, laterally accreting channels that are intercalated with continental deposits. IHS deposition occurred in both the brackish and freshwater parts of the depositional system.

2 IHS generation was controlled by tidal and seasonal factors. Several superimposed time cycles were recognized including semi-diurnal, fortnightly, monthly, semi-annual and annual cycles. The relative importance of these temporal controls varied in a distal–proximal gradient. Specifically, the tidal imprint was best observed from mesohaline to low and/or fluctuating salinity settings, whereas the seasonal control occurred in every part of the depositional system. The latter was most apparent in riverine channels close to the fluvio-tidal transition. Tidally dominated IHS formed cyclic rhythmites. In addition, seasonal IHS produced statistically verified non-random successions in a strongly tidally influenced setting.

3 The ancient tidal regime was semi-diurnal at Acre. Tidal ranges probably reached mesotidal conditions.

4 The asymmetry of adjacent couplets is generally regarded as a typical feature of tidally dominated environments. However, a strong asymmetry can develop in adjacent seasonal couplets in a near-equatorial setting; this is interpreted as being due to a double rainy season caused by equinoctial rains.

5 The different temporal controls commonly have distinguishable impact on sedimentological and ichnological properties. The differing properties include: lateral variability in lithology and bedforms in IHS, lateral continuity of IHS, contacts of the IHS members, thickness variation of IHS members within a set, cyclicities in IHS series, bioturbation degree and ichnofabric structure vs. couplet thickness, distribution of bioturbation in adjacent IHS members and change in genera composition and trace fossil behaviour in adjacent IHS members.

ACKNOWLEDGEMENTS

We are grateful to Kathy Campbell, Allen Archer, and editors Paul Carling and Peter Haughton for their thorough reviews of the manuscript. Elaine Richardson kindly carried out proof-reading. Finally, we would like to thank the Academy of Finland for funding and Universidade Federal do Acre (UFAC) for their co-operation that made the study possible.

REFERENCES

Ainsworth, R.B. and **Walker, R.G.** (1994) Control of estuarine valley-fill deposition by fluctuations of relative sea-level, Cretaceous Bearpaw-Horseshoe Canyon transition, Drumheller, Alberta, Canada. In: *Incised-Valley Systems: Origin and Sedimentary Sequences* (Eds R.W. Dalrymple, R. Boyd and B.A. Zaitlin), *SEPM Spec. Publ.*, **51,** 159–174.

Allen, J.R.L. (1968) *Current Ripples. Their Relation to Patterns of Water and Sediment Motion.* North-Holland Publishing Company, Amsterdam, 433 pp.

Archer, A.W. (1998) Hierarchy of controls on cyclic rhythmite deposition: Carboniferous basins of eastern and mid continental USAIn: *Tidalites: Processes and Products* (Eds C.R. Alexander, R.A. Davis and V.J. Henry), *SEPM Spec. Publ.*, **61,** 59–68.

Archer, A.W. (2005) Review of Amazonian depositional systems. In: *Fluvial Sedimentology VII* (Eds M. Blum, S. Marriott and S. Leclair), *Spec. Publ. Int. Assoc. Sed.*, **35,** 17–39.

Barwish, J.H. (1978) Sedimentology of some South Carolina tidal creek point bars, and a comparison with their fluvial counterparts. In: *Fluvial Sedimentology* (Ed. A.D. Miall), *Can. Soc. Petrol. Geol. Mem.*, **5,** 129–160.

Bechtel, D.J., Yuill, C.N., Ranger, M.J. and **Pemberton, S.G.** (1994) *Ichnology of Inclined Heterolithic Stratification of the McMurray Formation, Northeastern Alberta*. C.S.P.G. Mannville Core Conference, pp. 351–368.

de Boer, P.L., Oost, A.P. and **Visser, M.J.** (1989) The diurnal inequality of the tide as a parameter for recognizing tidal influences. *J. Sed. Petrol.*, **59,** 912–921.

Brito, P.M. and **Deynat, P.P.** (2004) Freshwater stingrays from the Miocene of South America with comments on the rise of potamotrygonids (Batoidea, Myliobatiformes). In: *Recent Advances in the Origin and Early Radiation of Vertebrates* (Eds G. Arratia, M.V.H. Wilson and R. Cloutier), Verlag Dr. Friedrich Pfeil, München, Germany, pp. 575–582.

Campbell, K.E., Heizler, M., Frailey, C.D., Romero-Pittman, L. and **Prothero, D.R.** (2001) Upper Cenozoic chronostratigraphy of the southwestern Amazon Basin. *Geology*, **29,** 595–598.

Carvalho, P., Bocquentin, J. and **Lapparent de Droin, F.** (2002) A new species Podocnemis (Pleurodira, Podocnemididae) from the Neogene of the Solimões Formation, Acre, Brazil. *Geobios*, **35,** 677–686.

Choi, K., Dalrymple, R., Chun, S. and **Kim, S.-P.** (2004) Sedimentology of modern, inclined heterolithic stratification (IHS) in the Macrotidal Han River Delta, Korea. *J. Sed. Res.*, **74,** 677–689.

Dalrymple, R.W., Zaitlin, B.A. and **Boyd, R.** (1992) Estuarine facies models: conceptual basis and stratigraphic implications. *J. Sed. Petrol.*, **62,** 1130–1146.

Dalrymple, R.W., Baker, E.K., Harris, P.T. and **Hughes, M.G.** (2003) Sedimentology and stratigraphy of a tide-dominated, foreland basin delta (Fly River, Papua New Guinea). In: *Tropical Deltas of Southeast Asia – Sedimentology, Stratigraphy and Petroleum Geology* (Eds H. Sidi, D. Nummedal, P. Imbert, H. Darman and H.W. Posamentier), *SEPM Spec. Publ.*, **76,** 147–173.

Frailey, C.D. (1986) Late Miocene and Holocene Mammals, exclusive of the Notoungulata, of the Rio Acre Region, Western Amazonia. Contributions in Science. *Nat. Hist. Mus. Los Angeles County*, **374,** 1–46.

Gingras, M.K., Pemberton, S.G., Saunders, T. and **Clifton, H.E.** (1999) Ichnology of modern and Pleistocene brackish-water deposits at Willapa Bay, Washington: variability in estuarine settings. *Palaios*, **14,** 352–374.

Gingras, M.K., Räsänen, M.E. and **Ranzi, A.** (2002) The significance of bioturbated inclined heterolithic stratification in the southern part of the Miocene Solimões Formation, Rio Acre, Amazonia Brazil. *Palaios*, **17,** 591–601.

Greb, S.F. and **Archer, A.W.** (1998) Annual sedimentation cycles in rhythmites of Carboniferous tidal channels. In: *Tidalites – Processes and Products* (Eds C.R. Alexander, R.A. Davis and V.J. Henry), *SEPM Spec. Publ.*, **61,** 75–83.

Hasiotis, S. (2003) Complex ichnofossils of solitary and social soil organisms: understanding their evolution and roles in terrestrial palaeoecosystems. *Palaeogeogr. Palaeoclimatol. Palaeoecol.*, **192,** 259–320.

Hermoza, W. (2004) *Dynamique tectono-sédimentaire et restauration séquentielle du retro-bassin d'avant-pays des Andes centrales*. PhD thesis. University of Paul Sabatier de Toulouse III, 296 pp.

Hernández, R., Jordan, T., Dalentz, Farjat, A., Echavarría, L., Idleman, B. and **Reynolds, J.** (2005) Age, distribution, tectonics and eustatic controls of the Paranense and Caribbean marine transgressions in southern Bolivia and Argentina. *J. S. Am. Earth Sci.*, **19,** 495–512.

Hoorn, C. (1994) *Miocene palynostratigraphy and palaeoenvironments of northwestern Amazonia: Evidence of marine incursions and the influence of Andean tectonics*. PhD thesis. University of Amsterdam, Amsterdam, the Netherlands, 156 pp.

Hoorn, C. (1996) Late Miocene tidal deposits in the Amazonian foreland basin: Comment. *Science*, **273,** 122.

Hoorn, C. (2006) Mangrove Forests and Marine Incursions in Neogene Amazonia (Lower Apaporis River, Colombia). *Palaios*, **21,** 197–209.

Hovikoski, J., Räsänen, M., Gingras, M., Roddaz, M., Brusset, S., Hermoza, W., Romero-Pittman, L. and **Lertola, K.** (2005) Miocene semidiurnal tidal rhythmites in Madre de Dios, Peru. *Geology*, **33,** 177–180.

Hovikoski, J., Räsänen, M., Gingras, M., Lopez, S., Romero, L., Ranzi, A. and **Melo, J.** (2007) Palaeogeographical implications of the Miocene Quendeque Formation (Bolivia) and tidally-influenced strata in the southwestern Amazonia. *Palaeogeogr. Palaeoclimatol. Palaeoecol.*, **243,** 23–41.

Kaandorp, R.J.G., Vonhof, H.B., Wesselingh, F.P., Romero Pittman, L., Kroon, D. and **van Hinte, J.E.** (2005) Seasonal Amazonian rainfall variation in the Miocene Climate Optimum. *Palaeogeogr. Palaeoclimatol. Palaeoecol.*, **221,** 1–6.

Kummel, B. (1948) Geological reconnaissance of the Contamana Region, Peru. *Geol. Soc. Am. Bull.*, **69,** 1217–1266.

Kvale, E.P. and **Mastalerz, M.** (1998) Evidence of ancient freshwater tidal deposits. In *Tidalites: Processes and Products* (Eds C.R. Alexander, R.A. Davis and V.J. Henry), *SEPM Spec. Publ.*, **61,** 95–107.

Latrubesse, E.M., Bocquentin, J., Santos, J.R. and **Ramonell, C.G.** (1997) Palaeoenvironmental model for the late Cenozoic of southwestern Amazonia: palaeotology and geology. *Acta Amazonica*, **27,** 103–118.

Lettley, C.D. (2004) *Elements of a Genetic Framework for Inclined Heterolithic Strata of the McMurray Formation, Northeast Alberta*. Unpublished master thesis. University of Alberta, Canada, 150 pp.

McGregor, G.R. and **Nieuwolt, S.** (1998) *Tropical Climatology – An Introduction to the Climates of the Low Latitudes*. John Wiley & Sons, Chichester, 339 pp.

Mossop, G.D. (1975) Epsilon cross-strata in the Athabasca oil sands. In: *Fluvial Sedimentology*. (Ed. A.D. Miall), *Can. Soc. Petrol. Geol. Mem.*, **5,** 854.

Nesbitt, E. and **Campbell, K.** (2006) The Palaeoenvironmental Significance of Psilonichnus. *Palaios*, **21,** 187–196.

Oppenheim, V. (1946) Geological reconnaissance in southeastern Peru. *Geological Society of America Bulletin*, **30,** 254–264.

Page, K., Nanson, G. and **Frazier, P.** (2003) Floodplain formation and sediment stratigraphy resulting from oblique accrection on the Murrumbidgee River, Australia. *Journal of Sedimentary Research*, **73,** 5–14.

Paxton, C.G.M. and **Crampton, W.G.R.** (1996) Technical comments. *Science*, **273,** 123.

Pollard, J.E., Goldring, R. and **Buck, S.G.** (1993) Ichnofabrics containing *Ophiomorpha:* significance in shallow water facies interpretation. *J. Geol. Soc. London*, **150,** 149–164.

Räsänen, M.E., Linnea, A., Irion, G., Rebeta, H., Wesselingh, F. and **Vargas, R.** (1998) Geología y geoformas de la zona de Iquitos. In: Geoecología y desarrollo Amazónico. Estudio integrado en la zona de Iquitos, Perú (Eds R. Kalliola and S. Flores), *Annales Universitatis Turkuensis Ser. A II*, **114,** 59–137.

Räsänen, M.E., Linna, A.M., Santos, J.C.R. and **Negri, F.R.** (1995) Late Miocene tidal deposits in the Amazonian foreland basin. *Science*, **269**, 386–390.

Rebata, L., Gingras, M., Räsänen, M. and **Barberi, M.** (2006) Tidal-channel deposits on a delta plain from the Upper Miocene Nauta formation, Marañon Foreland Sub-basin, Peru. *Sedimentology*, **53**, 971–1013.

Roddaz, M., Baby, P., Brusset, S., Hermoza, W. and **Darrozes, J.M.** (2005a) Forebulge dynamics and environmental control in Western Amazonia: the case study of the Arch of Iquitos (Peru). *Tectonophysics*, **399**, 87–108.

Roddaz, M., Viers, J., Brusset, S., Baby, P. and **Herail, G.** (2005b) Sediment provenances and drainage evolution of the Neogene Amazonian foreland basin. *Earth Planet. Sci. Lett.*, **239**, 57–78.

Roddaz, M., Brusset, S., Baby, P. and **Hérail, G.** (2006) Miocene tidal-influenced sedimentation to continental Pliocene sedimentation in the forebulge-backbulge depozones of the Beni-Mamore foreland basin (northern Bolivia). *J. S. Am. Earth Sci.*, **20**, 351–368.

Schobbenhaus, C.D., de Campos, A., Derze, G.R. and **Asmus, H.E.** (1984) *Geologia do Brasil.* DNPM, Brasília, 501 pp.

Siiro, P., Räsänen, M., Gingras, M., Harris, C., Irion, G., Pemberton, S.G. and **Ranzi, A.** (2005) Application of laser diffraction grain-size analysis to reveal depositional processes in tidally-influenced systems. In: *Fluvial Sedimentology VII* (Eds M. Blum, S. Marriott and S. Leclair), *Int. Assoc. Sedimentol. Spec. Publ.*, **35**, 159–180.

Smith, D.G. (1988) Modern point bar deposits analogous to the Athabasca oil sands. In: *Tide-Influenced Sedimentary Environments and Facies* (Eds P.L. de Boer, A. van Gelder and S.D. Nio), D. Reidel Publ. Co., Dordrecht, 417–432.

Thomas, R.G., Smith, D.G., Wood, J.M., Visser, J., Calverly-Range, E.A. and **Koster, E.H.** (1987) Inclined heterolithic stratification; terminology, description, interpretation and significance. *Sed. Geol.*, **53**, 123–179.

Van den Berg, J.H. (1981) Rhythmic seasonal layering in a mesotidal channel fill sequences, Oosterschelde Mouth, the Netherlands. In: *Holocene Marine Sedimentation in the North Sea Basin* (Eds S.D. Nio, R.T.E. Shuttenhelm and T.C.E. Van Weering), *Int. Assoc. Sedimentol. Spec. Publ.*, **5**, 147–159.

Wells, M.R., Allison, P.A., Hampson, G.J., Piggot, M.D. and **Pain, C.C.** (2005) Modelling ancient tides: the Upper Carboniferous epi-continental seaway of Northwest Europe. *Sedimentology*, **52**, 715–735.

Wesselingh, F. (2003) *A Miocene faunule from Madre de Dios (Peru).* Internal report, 172, Division of Cenozoic Mollusca, Nationaal Natuurhistorisch Museum Naturalis, Leiden, Netherlands, 4 pp.

Westaway, R. (2006) Late Cenozoic sedimentary sequences in Acre state, southwestern Amazonia: Fluvial or tidal?: Deductions from the IGCP 449 fieldtrip. In: *New Contributions on Neogene Geography and Depositional Environments in Amazonia* (Eds C. Hoorn and H. Vonhof), *J. S. Am. Earth Sci.*, **21**, 120–134.

Manuscript received 24 August 2005; revision accepted 20 August 2007